

# FAST ACCRETION OF SMALL PLANETESIMALS BY PROTOPLANETARY CORES.

R. R. RAFIKOV

IAS, Einstein Dr., Princeton, NJ 08540

*Draft version September 10, 2018*

## ABSTRACT

We explore the dynamics of small planetesimals coexisting with massive protoplanetary cores in a gaseous nebula. Gas drag strongly affects the motion of small bodies leading to the decay of their eccentricities and inclinations, which are excited by the gravity of protoplanetary cores. Drag acting on larger ( $\gtrsim 1$  km), high velocity planetesimals causes a mere reduction of their average random velocity. By contrast, drag qualitatively changes the dynamics of smaller ( $\lesssim 0.1 - 1$  km), low velocity objects: (1) small planetesimals sediment towards the midplane of the nebula forming vertically thin subdisk; (2) their random velocities rapidly decay between successive passages of the cores and, as a result, encounters with cores typically occur at the minimum relative velocity allowed by the shear in the disk. This leads to a drastic increase in the accretion rate of small planetesimals by the protoplanetary cores, allowing cores to grow faster than expected in the simple oligarchic picture, provided that the population of small planetesimals contains more than roughly 1% of the solid mass in the nebula. Fragmentation of larger planetesimals ( $\gtrsim 1$  km) in energetic collisions triggered by the gravitational scattering by cores can easily channel this amount of material into small bodies on reasonable timescales ( $< 1$  Myr in the outer Solar System), providing a means for the rapid growth (within several Myr at 30 AU) of rather massive protoplanetary cores. Effects of inelastic collisions between planetesimals and presence of multiple protoplanetary cores are discussed.

*Subject headings:* planetary systems: formation — solar system: formation — Kuiper Belt

## 1. INTRODUCTION.

Formation of terrestrial planets and solid cores of giant planets is thought to proceed via the gravity-assisted merging of a large number of planetesimals — solid bodies with initial sizes of roughly several kilometers. Despite a considerable progress made in this field since the pioneering works of Safronov (1969), a number of important problems still remain unsolved. One of the most serious questions has to do with the time needed for planets to complete their growth to present sizes. In the framework of conventional theory this time is rather long, especially in the outer parts of the protoplanetary nebula ( $\gtrsim 10^8 - 10^9$  yr), and it is likely that the gaseous component of the nebula dissipates much earlier (in  $\lesssim 10^6 - 10^7$  yr). This would make it very hard for the giant planets in our Solar System to accrete their huge gaseous envelopes via core instability (Mizuno 1980) which is otherwise considered to be an attractive scenario.

Wetherill & Stewart (1989) have identified a very rapid “runaway” regime of accretion of protoplanetary cores which at the time seemed like a solution of this problem. However, later on Ida & Makino (1993) and Kokubo & Ida (1996, 1998) have demonstrated that the runaway accretion would persist only through a rather limited interval of time and that the final growth of protoplanetary cores to isolation (which corresponds to roughly  $10^{26} - 10^{27}$  g at 1 AU) would proceed in a slow manner, making the formation of cores of giant planets rather problematic.

These studies usually implied that the gaseous component of the nebula plays only a secondary role in the planet formation process. Planetesimals were typically assumed to be rather massive ( $10^{23} - 10^{24}$  g) bodies

weakly affected by the gas (Kokubo & Ida 1998). This allows gravity to excite energetic random motions of planetesimals leading to diminishing the role of gravitational focusing and reduction of accretion efficiency. The purpose of this paper is to relax this assumption and to see what impact is incurred on the planet formation picture by allowing most of the planetesimals to be small ( $\lesssim 10$  km) bodies immersed in a gaseous environment. Such planetesimals would be appreciably affected by the gas drag and we will demonstrate that this can bring qualitative changes to their dynamics in the vicinity of the protoplanetary cores and, consequently, to the behavior of the mass accretion rate of cores.

Throughout this study we will use the following approximation to the structure of the Minimum Mass Solar Nebula (MMSN):

$$\Sigma_g(a) \approx 100 \Sigma_p(a) \approx 3000 \text{ g cm}^{-2} a_{AU}^{-3/2}, \quad (1)$$

$$c_s(a) \approx 1.2 \text{ km s}^{-1} a_{AU}^{-1/4}, \quad (2)$$

where  $\Sigma_p, \Sigma_g$  are the particulate and gas surface densities correspondingly,  $c_s$  is the gas sound speed, and  $a_{AU} \equiv a/(1 \text{ AU})$  is a distance from the Sun  $a$  scaled by 1 AU. We will use the terms “protoplanetary core” and “protoplanetary embryo” interchangeably. Physical density of planetesimals  $\rho_p$  is always assumed to be  $1 \text{ g cm}^{-3}$ .

The paper is organized as follows: after a discussion of different gas drag regimes in §2 we proceed to the description of planetesimal dynamics in the vicinity of protoplanetary cores in §3. The inclination of small planetesimals, a question very important for this study, is explored in §3.4. The separation of different gas drag and dynamical regimes in different parts of the nebula is described in §3.5 and lower limits on the random velocities of planetesimals are obtained in §4. We dwell

upon the role of inelastic collisions between planetesimals in §5. The role of small planetesimals in the growth of protoplanetary cores is studied in §6 and some important consequences for the planet formation picture are discussed in §7.

## 2. SUMMARY OF DIFFERENT GAS DRAG REGIMES.

Drag force acting on a body moving in a gaseous medium depends on the relative velocity of the body with respect to the gas  $v_r$  and on the ratio of its radius  $r_p$  to the molecular mean free path  $\lambda$  (Whipple 1972; Weidenschilling 1977). Whenever  $r_p \lesssim \lambda$  the Epstein drag law applies:

$$\frac{d\mathbf{v}_r}{dt} \simeq -\frac{\rho_g c_s}{\rho_p r_p} \mathbf{v}_r \simeq -\Omega \frac{\Sigma_g}{\rho_p r_p} \mathbf{v}_r, \quad (3)$$

where  $\Omega$  is the angular frequency of the disk,  $\rho_g$  is the gas density,  $r_p$  is the planetesimal size, and  $\rho_p$  is the physical density of planetesimals (planetesimal random velocities are assumed to be subsonic). For the adopted MMSN model (2) we estimate

$$\lambda = (n_g \sigma_{H_2})^{-1} \simeq \frac{\mu c_s}{\Omega \Sigma_g \sigma_{H_2}} \simeq 1 \text{ cm } a_{AU}^{11/4} \quad (4)$$

for  $H_2$  collision cross section  $\sigma_{H_2} \simeq 10^{-15} \text{ cm}^2$  ( $\mu$  is the mean molecular weight). Here  $n_g$  is a number density of  $H_2$  molecules. It is important to notice that  $\lambda$  increases very rapidly with the distance from the Sun, so that although only sub-cm particles can experience Epstein drag at 1 AU, at 30 AU this drag regime is valid even for rocks 100 m in size!

A large spherical body with  $r_p \gtrsim \lambda$  experiences a deceleration of the form

$$\frac{d\mathbf{v}_r}{dt} \simeq -C_D \frac{3}{4\pi} \frac{\rho_g}{\rho_p r_p} v_r \mathbf{v}_r. \quad (5)$$

Drag coefficient  $C_D$  is a function of the Reynolds number  $Re \equiv v_r r_p / \nu$ , where  $\nu$  is a kinematic viscosity. The viscosity we assume here is the molecular viscosity, i.e.  $\nu \simeq \lambda c_s / 3$ ; in the presence of anomalous sources of viscosity the expression for  $\nu$  has to be correspondingly adjusted.

For  $Re \lesssim 1$  gas drag is in the Stokes regime (Landau & Lifshitz 1987), meaning that  $C_D = 6\pi Re^{-1}$ . For  $Re \gg 1$  drag coefficient becomes constant:  $C_D \simeq 0.7$  (Weidenschilling 1977). We neglect the more complicated behavior of  $C_D$  for  $1 \lesssim Re \lesssim 10^2$  (Whipple 1972) and simply assume that  $C_D$  switches from one asymptotic behavior to the other at  $Re_b \simeq 20$ . Thus, we adopt

$$\frac{d\mathbf{v}_r}{dt} \simeq -\frac{3}{2} \Omega \frac{\Sigma_g}{\rho_p r_p} \frac{\lambda}{r_p} \mathbf{v}_r, \quad Re \lesssim Re_b, \quad (6)$$

$$\frac{d\mathbf{v}_r}{dt} \simeq -0.2 \Omega \frac{\Sigma_g}{\rho_p r_p} \frac{v_r}{c_s} \mathbf{v}_r, \quad Re \gtrsim Re_b. \quad (7)$$

Separation of different gas drag regimes as a function of  $r_p$  and  $v_r$  is schematically presented in Figure 1.

Gas drag acting on a planetesimal moving on an elliptic and inclined orbit leads to the decay of planetesimal eccentricity  $e$ , inclination  $i$ , and semimajor axis  $a$  (Adachi et al. 1976). For the calculation of the decay rate of the orbital elements it is important to take into account the sub-Keplerian angular velocity of the gas in the nebula

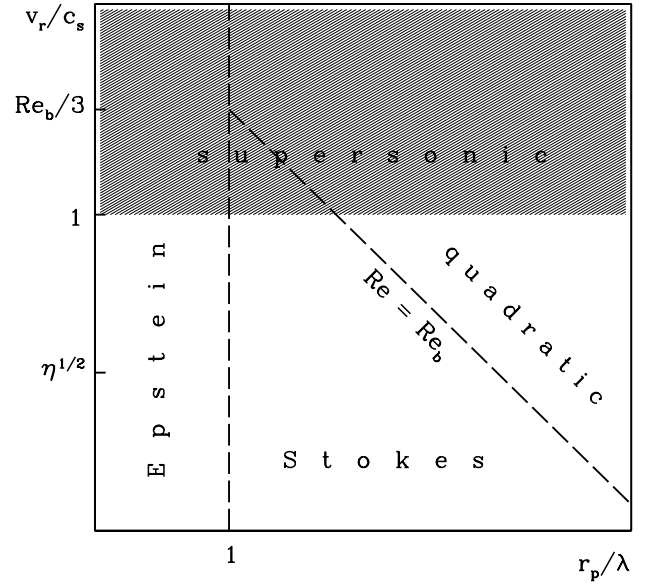


FIG. 1.— Separation of different gas drag regimes on  $r_p/\lambda - v_r/c_s$  plane. Dashed lines separate regions where different gas drag laws (indicated on a plot) apply. Planetesimals in the shaded part of the plot move supersonically with respect to the gas. Separation between the quadratic and Stokes regimes ( $Re = Re_b$ ) is determined by  $v_r/c_s = (Re_b/3)(r_p/\lambda)^{-1}$ .

caused by the radial pressure support. This gives rise to additional azimuthal contribution  $\Delta v_g$  to the relative gas-planetesimal velocity. One can easily demonstrate that (Whipple 1971)

$$\Delta v_g \approx \Omega a \left( \frac{c_s}{\Omega a} \right)^2 \equiv \Omega a \eta \simeq 50 \text{ m s}^{-1}, \quad (8)$$

$$\eta \equiv \left( \frac{c_s}{\Omega a} \right)^2 \simeq 1.6 \times 10^{-3} a_{AU}^{1/2}. \quad (9)$$

For our adopted temperature profile  $\Delta v_g$  is independent of  $a$ . Whenever random velocity of planetesimal exceeds  $\Delta v_g$  this velocity offset provides only a small contribution to the relative gas-planetesimal velocity. In the opposite case relative velocity is dominated by  $\Delta v_g$ .

Using (3)-(7) we can introduce a *damping time*  $t_d$  — typical time needed to decelerate planetesimals by the gas drag if their initial velocity with respect to the gas is  $\Delta v_g$ . Using equations (3), (6), & (7) one obtains

$$t_d \approx 5 \Omega^{-1} \frac{\rho_p r_p}{\Sigma_g} \frac{\Omega a}{c_s}, \quad (10)$$

$$t_d \approx \frac{2}{3} \Omega^{-1} \frac{\rho_p r_p}{\Sigma_g} \frac{r_p}{\lambda}, \quad (11)$$

$$t_d \approx \Omega^{-1} \frac{\rho_p r_p}{\Sigma_g} \quad (12)$$

for the quadratic, Stokes, and Epstein drag regimes respectively.

When  $t_d \ll \Omega^{-1}$  planetesimal motion is tightly coupled to that of the gas; critical planetesimal size  $r_{stop}$  at which the transition from almost Keplerian motion to the sub-Keplerian gas rotation occurs can be determined from

the condition  $t_d \approx \Omega^{-1}$ . Using (10)-(12) we find that

$$r_{stop} \approx 0.2 \frac{\Sigma_g}{\rho_p} \frac{c_s}{\Omega a} \approx 20 \text{ cm } a_{AU}^{-5/4}, \quad (13)$$

$$r_{stop} \approx \left( \frac{3}{2} \frac{\Sigma_g}{\rho_p} \lambda \right)^{1/2} \approx 70 \text{ cm } a_{AU}^{5/8}, \quad (14)$$

$$r_{stop} \approx \frac{\Sigma_g}{\rho_p} \approx 3 \times 10^3 \text{ cm } a_{AU}^{-3/2}, \quad (15)$$

for the quadratic, Stokes, and Epstein drag regimes.

Calculation of the orbital evolution of planetesimals bigger than  $r_{stop}$  due to gas drag was performed by Adachi et al. (1976; see also Tanaka & Ida 1997) taking into account the saturation of the relative gas-planetesimal velocity whenever the planetesimal random speed is  $\lesssim \Delta v_g$ . We quote their results for different drag regimes keeping only the most important contributions<sup>1</sup>:

$$\frac{1}{e^2} \frac{de^2}{dt} \approx \frac{2}{i^2} \frac{di^2}{dt} \approx -0.2 \Omega \frac{\Sigma_g}{\rho_p r_p} \frac{\Omega a}{c_s} (e + i + \eta), \quad (16)$$

$$\frac{1}{a} \frac{da}{dt} \approx -0.2 \Omega \frac{\Sigma_g}{\rho_p r_p} \frac{\Omega a}{c_s} \eta (e + i + \eta), \quad (17)$$

for the quadratic dependence (7) of gas drag on velocity. The decay rates represented by equations (16) & (17) behave differently for  $e, i \lesssim \eta$  and  $e, i \gtrsim \eta$ . In the first case the relative gas-planetesimal velocity is close to  $\Delta v_g$ ; as a result, orbital elements exponentially decay with time. In the second case  $v_r$  is dominated by the planetesimal random motion and the decay time is inversely proportional to the random velocity  $v \approx (e + i)\Omega a$ .

For the linear dependence of gas drag on  $v_r$  represented by the equations (3) and (6) one finds (Adachi et al. 1976)

$$\frac{1}{e^2} \frac{de^2}{dt} \approx \frac{2}{i^2} \frac{di^2}{dt} \approx -\Omega \zeta \frac{\Sigma_g}{\rho_p r_p}, \quad (18)$$

$$\frac{1}{a} \frac{da}{dt} \approx -\Omega \zeta \frac{\Sigma_g}{\rho_p r_p} \eta, \quad (19)$$

where  $\zeta = 1$  for  $r_p \lesssim \lambda$  (Epstein drag [3]), and  $\zeta = (3/2)\lambda/r_p$  for  $\lambda \lesssim r_p$ ,  $Re \lesssim Re_b$  (Stokes drag [6]).

### 3. SCATTERING BY MASSIVE PROTOPLANETARY CORES.

Let us consider the scattering of a planetesimal by a single protoplanetary core moving on a circular and uninclined orbit. The velocity perturbation which planetesimal receives in the course of gravitational interaction depends on the separation of the planetesimal guiding center from the embryo's orbit and on the planetesimal approach velocity  $v_a$ .

It is well known (Hénon & Petit 1986) that the Hill radius  $R_H$  of interacting bodies sets an important length scale for scattering in the disk. For two bodies with masses  $m_1$  and  $m_2$  Hill radius is defined as

$$R_H \equiv a \left( \frac{m_1 + m_2}{M_\odot} \right)^{1/3}. \quad (20)$$

<sup>1</sup> We have set to unity all numerical factors which appear in the course of orbital averaging; however we kept initial factors since some of them (e.g. in [7]) are significantly different from unity.

In the case of scattering of planetesimals by a protoplanetary embryo having mass  $M_e$  Hill radius is determined solely by  $M_e$ :  $R_H = a(M_e/M_\odot)^{1/3}$ .

For our purposes the planetesimal approach velocity can be represented as  $v_a \approx \Omega(ea + ia + R_H)$  and it is different from the horizontal random velocity  $v_h \equiv e\Omega a$  and vertical random velocity  $v_z \equiv i\Omega a$ . Additional contribution to  $v_a$  in the form of the shear across the Hill radius  $\Omega R_H$  (sometimes called the Hill velocity) appears because of the differential rotation of the disk. Gravitational focusing of planetesimals by the embryo is determined by  $v_a$ . Velocity  $v_z$  determines the vertical thickness of planetesimal disk, thus it regulates the volume number density of planetesimals  $n_p$  for a given surface mass density  $\Sigma_p$ :  $n_p = \Omega \Sigma_p / (v_z m_p)$ , where  $m_p \equiv (4\pi/3)\rho_p r_p^3$  is a planetesimal mass. Vertical velocity is much smaller than either  $v_a$  or the total random velocity  $v \approx v_h + v_z$  when  $i \ll e$ .

Whenever random velocity  $v$  is less than  $\Omega R_H$  — the so-called *shear-dominated* regime (Ida 1990) — close approaches between gravitationally interacting bodies which might lead to their physical collision are only possible for the orbital separation  $h \sim R_H$ . For  $h \gg R_H$  (distant encounters) orbital perturbations incurred in the course of scattering are small: changes of the random velocity  $\Delta v$  and of the orbital separation  $\Delta h$  produced by a *single* scattering have magnitudes

$$\Delta v \approx \Omega R_H (R_H/h)^2, \quad \Delta h \approx R_H (R_H/h)^2. \quad (21)$$

These increments can be positive or negative depending on the orbital phases of bodies and their random velocities before the encounter. The averages of these quantities over epicyclic phases were calculated by Hasegawa & Nakazawa (1990) and we quote here their result for the eccentricity (it will be used in §4):

$$\langle \Delta(e^2) \rangle \approx 5 (R_H/a)^2 \left( \frac{R_H}{h} \right)^4. \quad (22)$$

In the case  $h \sim R_H$ , when interacting bodies enter their mutual Hill sphere, strong scattering takes place:

$$\Delta v \approx \Omega R_H, \quad \Delta(h^2) \approx R_H^2, \quad (23)$$

with both increments being positive — orbits are repelled and random velocity  $\sim \Omega R_H$  is excited. At the same time, it is clear from purely geometrical considerations that for  $v \ll \Omega R_H$  the change of the vertical velocity is proportional to the vertical projection of the random velocity perturbation, and is much smaller than the change in the horizontal velocity:

$$\Delta v_z \sim \Delta v \frac{v_z}{v_a} \approx v_z, \quad \text{or} \quad \Delta i \sim i. \quad (24)$$

Since the total velocity increment  $\Delta v$  is of the order or bigger than the initial random velocity of planetesimals, scattering for  $h \sim R_H$  in the shear-dominated regime has a *discrete* character.

Another possible dynamical state of planetesimals is the *dispersion-dominated* regime which takes place whenever  $v \gtrsim \Omega R_H$ . In this case the epicyclic excursions of planetesimals allow collisions between the bodies with orbits separated by  $h < v/\Omega$ ; more distant bodies are again subject to only weak scattering. Moreover, even particles having close approaches experience *on average* only small

velocity perturbation compared to the pre-encounter velocity  $v_a$ . This allows one to treat the scattering in the dispersion-dominated regime as a *continuous* process, unlike the discrete scattering in the shear-dominated regime. Another important feature of the dispersion-dominated case is that  $v_z \sim v_h$ , or  $i \sim e$ , as a result of roughly three-dimensional nature of scattering in this regime which tends to isotropize highly anisotropic velocity distributions (Ida, Kokubo, & Makino 1993; Rafikov 2003c). Thus, it is enough to follow the evolution of only one component of planetesimal velocity (e.g.  $e$ ) in the dispersion-dominated regime.

### 3.1. Quadratic drag.

Let's now proceed to considering planetesimal dynamics for different gas drag regimes. First, we explore the case of quadratic drag represented by equations (7), (16), and (17) which is valid for  $r_p \gtrsim \lambda$ ,  $Re \gtrsim Re_b$ . This situation would most likely be realized in the inner parts of the protoplanetary nebula since  $\lambda$  is rather small there making Epstein regime irrelevant and bringing Reynolds number to a high value.

We first assume that scattering occurs in the dispersion-dominated regime and try to figure out under which conditions a steady state can be realized in this case. Gravitational scattering by the embryo increases planetesimal random energy at a rate<sup>2</sup> (Ida & Makino 1993; Rafikov 2003b)

$$\frac{dv^2}{dt} \approx \Omega(\Omega R_H)^2 \frac{R_H}{a} \left( \frac{\Omega R_H}{v} \right)^3 \ln \Lambda, \quad (25)$$

where  $\ln \Lambda \sim 1$  is a Coulomb logarithm and  $\Lambda \sim (v/\Omega R_H)^3$  for  $e \sim i \gtrsim R_H/a$  (Stewart & Ida 2000). Because of the very weak dependence of  $\ln \Lambda$  on velocity we will set it to unity in our further discussion.

Balancing this growth rate by the damping due to the gas drag (equation [16]) we find that

$$\begin{aligned} v &\approx \Omega R_H \left( 5 \frac{c_s}{\Omega a} \frac{\rho_p r_p}{\Sigma_g} \right)^{1/6} \\ &\approx 1.4 \Omega R_H \left( \frac{r_p}{1 \text{ km}} \right)^{1/6} a_{AU}^{7/24}, \quad \text{for } v \gtrsim \Delta v_g, \quad (26) \\ v &\approx \Omega R_H \left( 5 \frac{c_s}{\Omega a} \frac{\rho_p r_p}{\Sigma_g} \frac{R_H}{\eta a} \right)^{1/5} \\ &\approx 1.5 \Omega R_H \left( \frac{r_p}{1 \text{ km}} \right)^{1/5} \left( \frac{M_e}{10^{25} \text{ g}} \right)^{1/15} a_{AU}^{1/4}, \\ &\quad \text{for } v \lesssim \Delta v_g. \quad (27) \end{aligned}$$

For further convenience we normalize the embryo's mass  $M_e$  to a fiducial mass  $M_f$  and planetesimal radius to a fiducial radius  $r_f$  which are defined as

$$M_f \equiv M_\odot \eta^3 \simeq 8 \times 10^{24} \text{ g } a_{AU}^{3/2}, \quad (28)$$

$$r_f \equiv 0.2 \frac{\Sigma_g \Omega a}{\rho_p c_s} = 0.2 a \frac{\rho_g}{\rho_p} \simeq 150 \text{ m } a_{AU}^{-7/4}. \quad (29)$$

These two parameters uniquely characterize the dynamics of the embryo-planetesimal scattering when the gas

drag dependence on the velocity is represented by equation (7). Using this notation we conclude from (26) that  $v \gtrsim \Omega R_H$  and  $v \gtrsim \Delta v_g$  if

$$r_p/r_f \gtrsim 1, \quad (30)$$

$$M_e/M_f \gtrsim (r_p/r_f)^{-1/2}. \quad (31)$$

From (27) we find that  $v \gtrsim \Omega R_H$  and  $v \lesssim \Delta v_g$  if

$$M_e/M_f \gtrsim (r_p/r_f)^{-3}, \quad (32)$$

$$M_e/M_f \lesssim (r_p/r_f)^{-1/2}. \quad (33)$$

Thus, conditions (30) and (32) determine the region in the parameter space  $M_e - r_p$  in which planetesimals are dispersion-dominated with respect to embryo and maintain a steady-state velocity dispersion, see Figure 4.

Whenever both (30) and (32) are not fulfilled, scattering of planetesimals proceeds in the shear-dominated regime. As we have previously mentioned, this type of interaction has a discrete nature — gas drag causes significant evolution of planetesimal velocity between close approaches to the embryo. We consider a planetesimal initially separated in semimajor axis from the embryo by  $h \sim R_H$  with initial random velocity  $v \lesssim \Omega R_H$ . Immediately after scattering  $v$  increases to  $\sim \Omega R_H$ , and the post-scattering value of planetesimal eccentricity is  $e_0 \sim R_H/a = \eta(M_e/M_f)^{1/3}$ .

We will see in §3.4 that the inclination of planetesimals interacting with the embryo in the shear-dominated regime is typically much smaller than their eccentricity. Then we can easily solve equation (16) with initial condition  $e(0) = e_0$  to obtain a general solution in the form

$$e(t) \approx \eta \left[ (1 + \eta/e_0) \exp \left( \Omega t \eta \frac{r_f}{r_p} \right) - 1 \right]^{-1}. \quad (34)$$

For low-mass embryos,  $M_e \lesssim M_f$ , planetesimal velocity after shear-dominated scattering is always less than  $\Delta v_g$ , i.e.  $e_0 \lesssim \eta$ ; as a result, we find from (34) that  $v$  damps exponentially:

$$e(t) \approx e_0 \exp \left( -\Omega t \eta \frac{r_f}{r_p} \right) \approx \eta \left( \frac{M_e}{M_f} \right)^{1/3} e^{-t/t_d}. \quad (35)$$

Thus, eccentricity decays on a typical timescale  $t_d$ , see (10) & (29).

For high-mass embryos,  $M_e \gtrsim M_f$ , post-encounter velocity is above  $\Delta v_g$  ( $e_0 \gtrsim \eta$ ) and damping by the gas drag is very efficient:  $dv^2/dt \propto -v^3$ , see equation (7). One can find from (34) that in this case

$$e(t) \approx \frac{\eta}{(\eta/e_0) + \Omega t \eta (r_f/r_p)} = \frac{\eta}{(\eta/e_0) + (t/t_d)}, \quad (36)$$

for  $t \lesssim t_d$ . One finds that  $e$  drops to  $\eta$  after  $t \approx t_d$  independent of  $e_0$ . Beyond that point relative gas-planetesimal velocity is set by  $\Delta v_g$ , thus for  $t \gtrsim t_d$  eccentricity decays exponentially on a timescale  $t_d$ , analogous to (35). It also follows from (36) that significant reduction of eccentricity after scattering by the high mass embryo occurs already on a timescale  $t_d(\eta/e_0) \approx \Omega^{-1}(r_p/r_f)(a/R_H) \ll t_d$ .

Planetesimals radially separated from the embryo by  $\sim R_H$  pass the embryo's Hill sphere (and experience strong scattering) roughly every synodic period  $t_{syn}$  corresponding to the radial separation of  $R_H$ :

$$t_{syn} \approx \Omega^{-1}(a/R_H). \quad (37)$$

<sup>2</sup> In the dispersion-dominated regime  $v_a \approx v$ .

Requiring the damping time  $t_d$  to be shorter than  $t_{syn}$  (which is necessary for planetesimals to stay in the shear-dominated regime) for embryos less massive than  $M_f$  is equivalent to demanding that

$$\eta^{-1}(r_p/r_f) \lesssim a/R_H \quad \text{or} \quad M_e/M_f \lesssim (r_p/r_f)^{-3}. \quad (38)$$

Around more massive embryos with  $M_e \gtrsim M_f$  planetesimal eccentricity is strongly damped between consecutive encounters with the embryo below its initial value if  $t_d(\eta/e_0) \lesssim t_{syn}$  or if

$$(r_p/r_f)(a/R_H) \lesssim a/R_H \quad \text{or} \quad r_p/r_f \lesssim 1. \quad (39)$$

At the same time, eccentricity would not drop below  $\eta$  prior to the next encounter if (38) is not fulfilled simultaneously with (39).

Comparing (38) and (39) with the dispersion-dominated conditions (30) and (32) we see that depending on  $M_e/M_f$  and  $r_p/r_f$  there can only be two possible states in the system: (1) either planetesimals are scattered in a smooth, continuous fashion in the dispersion-dominated regime, with gas drag not capable of damping their eccentricities significantly between the consecutive approaches to the embryo, or (2) they are strongly scattered by the embryo in the shear-dominated regime at each approach and gas appreciably reduces their random velocities before the next encounter takes place.

The discrete nature of planetesimal scattering in the shear-dominated regime is very important for determining the approach velocity of planetesimals to the embryo. For example, if we were to assume that scattering in the shear-dominated regime is continuous (like in the dispersion-dominated case) the average rate of eccentricity growth would have had the form  $de/dt \sim (R_H/a)/t_{syn}$ , since embryo increases planetesimal eccentricity by  $\sim R_H/a$  every synodic period. Balancing this by the gas drag in the form (7), one would find the average value of eccentricity to be  $\sim (R_H/a)(t_d/t_{syn})$ . It would however be a grave mistake to assume that this is the eccentricity with which planetesimal approaches the embryo. Indeed, it follows from (35) that the planetesimal eccentricity right before the encounter with the embryo is  $\sim (R_H/a) \exp(-t_{syn}/t_d)$  for  $M_e \lesssim M_f$ , which is exponentially smaller than the average value of  $e$ ! Thus, proper treatment of the shear-dominated regime taking the discrete nature of scattering into account is crucial for figuring out the initial conditions of the interaction process. This will have important ramifications for the question of accretion of these planetesimals as we demonstrate in §6.

### 3.2. Stokes drag.

Planetesimals interact with the gas in the Stokes regime when  $r_p \gtrsim \lambda$  and  $Re \lesssim Re_b$ . The last condition depends not only on the particle size  $r_p$  but also on its velocity. We introduce another fiducial size,  $r_S$ , which is defined as a planetesimal size for which  $Re = Re_b$  at  $v = \Delta v_g$ :

$$r_S \equiv \lambda \frac{Re_b}{3} \frac{\Omega a}{c_s} \approx 2 \text{ m } a_{AU}^{5/2}. \quad (40)$$

Planetesimals with  $r_p \lesssim r_S$  always experience gas drag in the Stokes regime for  $M_p \lesssim M_f$  (because post-scattering planetesimal velocity is  $\lesssim \Delta v_g$ ,  $v_r \approx \Delta v_g$ , and  $Re \lesssim Re_b$ ).

Embryos more massive than  $M_f$  endow shear-dominated planetesimals with velocity  $\Omega R_H > \Delta v_g$  at each scattering episode. But even then planetesimals with sizes  $r_p \lesssim r_S$  satisfying condition

$$M_e/M_f \lesssim (r_p/r_S)^{-3} = \left(\frac{r_S}{r_f}\right)^3 (r_p/r_f)^{-3} \quad (41)$$

experience *only* the Stokes drag, i.e. their maximum velocity and physical size are never large enough for their Reynolds number to exceed  $Re_b$ . Planetesimals scattered by more massive embryos would experience quadratic drag right after the encounter (even if only temporarily) before switching to the Stokes regime. From equation (18) one can easily see that damping between encounters is purely exponential for the Stokes drag independent of the planetesimal velocity (similar to the quadratic drag for  $e \lesssim \eta$ , see §3.3.1).

Let us now turn to the dispersion-dominated regime. Balancing heating rate (25) by the damping rate (18) with  $\zeta = (3/2)\lambda/r_p$  we find that

$$\begin{aligned} v &\approx \Omega R_H \left[ \frac{2}{3} \left(\frac{M_e}{M_f}\right)^{1/3} \left(\frac{r_p}{r_f}\right)^2 \frac{r_f}{r_S} \right]^{1/5} \\ &\approx 5 \Omega R_H \left(\frac{r_p}{1 \text{ km}}\right)^{2/5} \left(\frac{M_e}{10^{25} \text{ g}}\right)^{1/15} a_{AU}^{-1/4}. \end{aligned} \quad (42)$$

Consequently, planetesimals are in the dispersion-dominated regime with respect to the embryo if

$$M_e/M_f \gtrsim \left(\frac{r_S}{r_f}\right)^3 (r_p/r_f)^{-6}. \quad (43)$$

Smaller planetesimals are in the shear-dominated regime and experience discrete scattering by the embryos. From equation (42) we also find that  $v \lesssim \Delta v_g$  whenever

$$M_e/M_f \lesssim \left(\frac{r_S}{r_f}\right)^{1/2} (r_p/r_f)^{-1}, \quad (44)$$

and that  $Re < Re_b$  (and drag is in the Stokes regime) if

$$M_e/M_f \lesssim \left(\frac{r_S}{r_f}\right)^3 (r_p/r_f)^{-7/2} \quad (45)$$

(see Figure 5). The last equation is a dispersion-dominated analog of the condition (41).

### 3.3. Epstein drag.

Smallest planetesimals with  $r_p \lesssim \lambda$ , are coupled to gas via the Epstein drag. Performing analysis analogous to that of §3.3.2 one finds that in the dispersion-dominated regime scattering by the embryo maintains planetesimal random velocity at the level of

$$\begin{aligned} v &\approx \Omega R_H \left[ \left(\frac{M_e}{M_f}\right)^{1/3} \frac{\lambda}{r_S} \frac{r_p}{r_f} \right]^{1/5} \\ &\approx 1.4 \Omega R_H \left(\frac{r_p}{1 \text{ km}}\right)^{1/5} \left(\frac{M_e}{10^{25} \text{ g}}\right)^{1/15} \left(\frac{a_{AU}}{30}\right)^{3/10} \end{aligned} \quad (46)$$

Planetesimals can only be in the dispersion-dominated regime with respect to the embryo if

$$M_e/M_f \gtrsim \left(\frac{r_S}{\lambda}\right)^3 (r_p/r_f)^{-3} \quad (47)$$

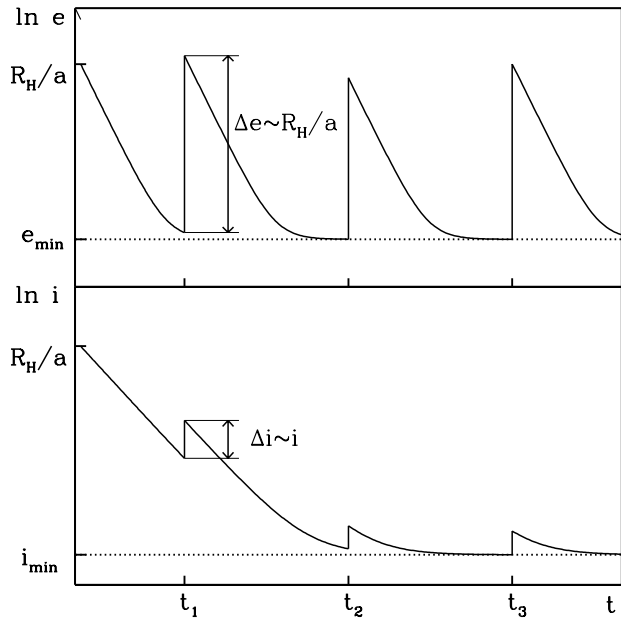


FIG. 2.— Sketch of the planetesimal eccentricity (*top*) and inclination (*bottom*) evolution due to the scattering by the embryo. Spikes correspond to close approaches to the embryo (which happen at different intervals because of the changing semimajor axis separation). We assume that there is a weak continuous source of planetesimal excitation keeping random velocities above some minimum level ( $e_{\min}$  and  $i_{\min}$ ). In reality behaviors of  $e$  and  $i$  are more erratic because of the scattering by distant embryos (see §4).

(see Figure 6). In this dynamical regime planetesimal velocity is below  $\Delta v_g$  only if

$$M_e/M_f \lesssim \left(\frac{r_S}{\lambda}\right)^{1/2} (r_p/r_f)^{-1/2}. \quad (48)$$

Planetesimals too small to satisfy (47) are in the shear-dominated regime and experience strong scattering by the embryo every synodic period, with their orbital elements exponentially decaying between encounters (analogous to the behavior in the case of Stokes drag, see §3.3.2).

#### 3.4. Inclination evolution.

It is easy to see from equations (16) and (18) that as long as gas drag is the only force affecting planetesimals after their encounter with embryo, planetesimal inclination decays according to

$$i(t) \approx i_0 \sqrt{e(t)/e_0}, \quad (49)$$

with  $e_0, i_0$  being the post-encounter values of eccentricity and inclination and  $e(t)$  given by (34) for quadratic gas drag. In the shear-dominated regime one might be tempted to think on the basis of (49) that  $i \gg e$  long after the encounter took place (when  $e \ll e_0$ ). This argument, however, assumes that  $i_0 \sim e_0$  and we now show that this is not the case.

Indeed, even if  $i_0 \sim R_H/a$ , inclination is exponentially small right before the next encounter (see [35] and [49]) since the damping time is shorter than the synodic period in the shear-dominated regime. After this second encounter, eccentricity increases to  $\sim R_H/a$ , while the

inclination does not go back to  $R_H/a$  but, according to (24), remains small, see Figure 2. Subsequent action of gas drag prior to the next passage of the core further reduces planetesimal inclination, and so on. As a result, we arrive at a very interesting conclusion: as long as planetesimals are in the shear-dominated regime their inclinations keeps decaying. Thus, all shear-dominated planetesimals “rain out” towards the disk midplane and collapse into geometrically thin layer. This emphasizes the importance of determining which part of the planetesimal population is shear-dominated with respect to the embryo.

Thickness of this layer would be zero if embryo were on purely uninclined orbit and gas drag were the only process affecting planetesimal dynamics between encounters. In reality, there are additional stirring agents which would keep the thickness of this subdisk finite (although still very small) and we consider them in §4 & §5.

#### 3.5. Separation of different regimes.

We now summarize what we have learned in §3.1-3.3 about planetesimal dynamics in the proto-Solar nebula.

First of all, it is clear from our previous discussion that the separation of different gas drag regimes sensitively depends on the relative values of fiducial planetesimal sizes  $\lambda$ ,  $r_f$ , and  $r_S$  given by the equations (4), (29), and (40). In Figure 3 we display the scaling of these sizes with the distance from the Sun. The boundary between the quadratic and Stokes drag regimes is calculated assuming  $v \approx \Delta v_g$  and coincides with  $r_S(a)$ . We also display the curve  $r_{\text{stop}}(a)$  using equations (13)-(15) — planetesimals with  $r_p$  below this curve (shaded region) are tightly coupled to the gas and their dynamics cannot be described by equations (16)-(19).

From Figure 3 one can see that depending on the location in the nebula there could be three possible situations: (a) when  $\lambda \lesssim r_S \lesssim r_f$ , which holds for  $a \lesssim 3$  AU in the MMSN, (b) when  $\lambda \lesssim r_f \lesssim r_S$ , which takes place for  $3 \text{ AU} \lesssim a \lesssim 9 \text{ AU}$ , and (c) when  $r_f \lesssim \lambda \lesssim r_S$ , which is valid for  $a \gtrsim 9 \text{ AU}$ .

The first case pertains to the region of terrestrial planets. We display possible regimes of planetesimal interaction with gas in this part of the nebula in Figure 4. They are classified according to the values of planetesimal size  $r_p$  and embryo mass  $M_e$ . Thick solid line separates planetesimals which interact with the embryo in the shear-dominated regime and experience discrete scattering (hatched region to the left of the curve) from those which undergo the dispersion-dominated scattering (unhatched region). In the terrestrial region, as we see from Figure 4, this curve is set by equations (30) and (32). Dashed curves denote the boundaries of different gas drag regimes: Epstein drag operates when  $r_p \lesssim \lambda$ ; Stokes drag operates whenever  $Re \lesssim Re_b$  — in the shear-dominated regime this implies  $r_p \lesssim r_S$  for embryos that cannot kick planetesimals by more than  $\Delta v_g$  ( $M_e \lesssim M_f$ , see §3.3.2), and restriction (41) for embryos that can<sup>3</sup> ( $M_e \gtrsim M_f$ ). For even bigger planetesimals gas drag is quadratic and

<sup>3</sup> In fact, even near embryos more massive than  $M_e$  determined from (41) planetesimals can spend some time in the Stokes regime: although they are in the quadratic drag regime right after the passage of the embryo, their velocity rapidly decreases after that and their Reynolds number can drop below  $Re_b$  before the next encounter takes place.

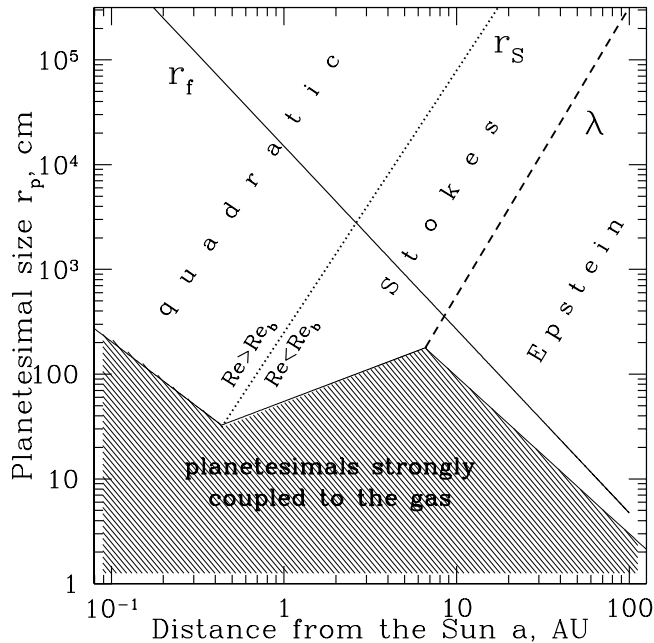


FIG. 3.— Behavior of the length scales  $r_f$ ,  $r_s$ , and  $\lambda$  important for the planetesimal interaction with the gas (with different regimes marked on the plot), as a function of distance  $a$  from the Sun. Planetesimals with sizes in the shaded region have stopping time shorter than local  $\Omega^{-1}$  and are thus moving together with the gas. Complex shape of the boundary of this region is due to the different gas drag regimes.

planetesimals can be either in the shear- (small ones) or in the dispersion-dominated (large ones) regime. In the latter regime the dot-dashed line separates cases of equilibrium planetesimal random velocity being higher or lower than  $\Delta v_g$ , see equations (31) and (33). When considering the population of small planetesimals we should always keep in mind that our discussion in §33.1-33.2 is valid only for planetesimals moving on almost Keplerian orbits. Thus, a condition  $r_p \gtrsim r_{stop}$  must be satisfied which restricts the validity of our results to planetesimals bigger than  $\sim 1$  m (see Figure 3). Smaller planetesimals largely follow the motion of the gas. Embryo's mass is not allowed to exceed  $\eta^{-3/2} M_f$  because more massive protoplanetary cores excite supersonic random velocities of surrounding planetesimals.

As we have demonstrated in §33.4 small shear-dominated planetesimals sediment into the geometrically thin subdisk (thinner than the embryo's Hill radius) near the midplane of the nebula. We can readily see from the Figure 4 that in the terrestrial region this destiny awaits all planetesimals smaller than  $\approx 100 - 200$  m in size (less than  $\sim 10^{13} - 10^{14}$  g in mass) in the vicinity of embryos more massive than about  $10^{25}$  g. Near less massive embryos even larger planetesimals can belong to this dynamically cold population: only bodies bigger than about 1 km can escape this fate near  $10^{23}$  g mass embryo. Thus, gas drag can have important effect even on 0.1 – 1 km size planetesimals when the question of their interaction with the massive embryos is concerned.

Figure 5 represents the separation of different gas drag and dynamical regimes at 5 AU from the Sun ( $\lambda \lesssim r_f \lesssim r_s$ ), corresponding to the giant planet region (roughly

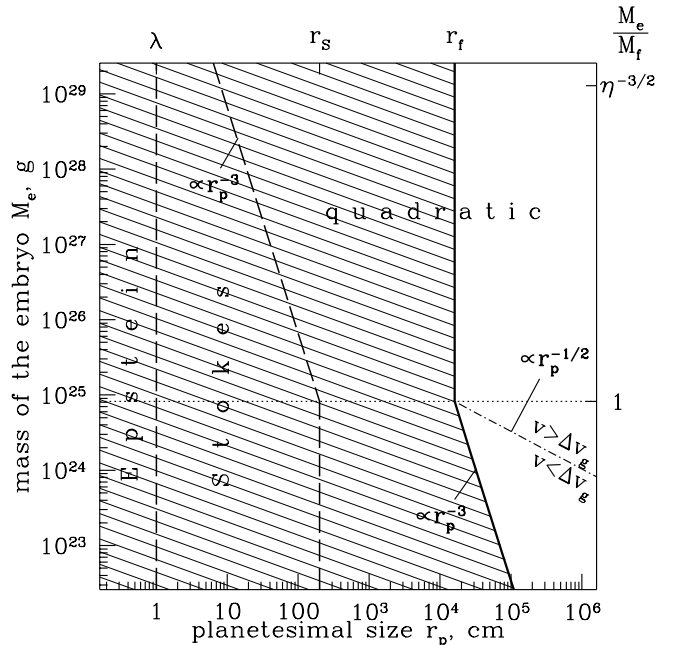


FIG. 4.— Separation of planetesimals into the shear- and dispersion-dominated ones with respect to the embryo in the phase space of the embryo's mass  $M_e$  and planetesimals size  $r_p$ . This particular separation and numerical values indicated in the Figure pertain  $a = 1$  AU (terrestrial planet region), where  $\lambda \lesssim r_s \lesssim r_f$ . Thick solid line separates two dynamical regimes, with shear-dominated one being hatched. Thick dashed curves separate different regimes of planetesimal interaction with the gas (explicitly indicated on the plot). See text for more details.

the semimajor axis of Jupiter). Again, one should keep in mind that planetesimal smaller than about 1 m are tightly coupled to the gas at 5 AU, see Figure 3. Evidently, the structure of the  $M_e - r_p$  phase space is more complex in this part of the nebula. For example, planetesimals interacting with the embryo in the dispersion-dominated regime can now experience not only quadratic but also the Stokes drag. The reason for this is the lower Hill velocity  $\Omega R_H$  for a given  $M_e$  at 5 AU which reduces the efficiency of planetesimal stirring by the embryo (see [25]) and diminishes the equilibrium planetesimal velocity. As a result, Reynolds number can drop below  $Re_b$  even for the dispersion-dominated planetesimals and drag can switch to the Stokes regime. Boundaries of different drag regimes are computed using equations (41) and (45). Hatched region again represents  $M_e$  and  $r_p$  for which planetesimal scattering by the embryo occurs in the shear-dominated regime (its boundary is determined by equations [30], [32], and [43]). One can see that this happens for planetesimals that are somewhat smaller than at 1 AU:  $r_p \lesssim 30$  m for  $M_e \approx 10^{26}$  g and  $r_p \lesssim 100$  m for  $M_e \approx 10^{23}$  g. This is because gas density rapidly drops with the distance from the Sun diminishing the strength of dissipation, and this tendency cannot be counteracted by the longer synodic period at 5 AU (for a given  $M_e$ ). Thus, somewhat less planetesimal material will be concentrated in the vertically thin subdisk of small bodies at 5 AU than at 1 AU, but the difference is not very pronounced.

Finally, Figure 6 displays the situation at 30 AU (roughly the semimajor axis of Neptune), in the region

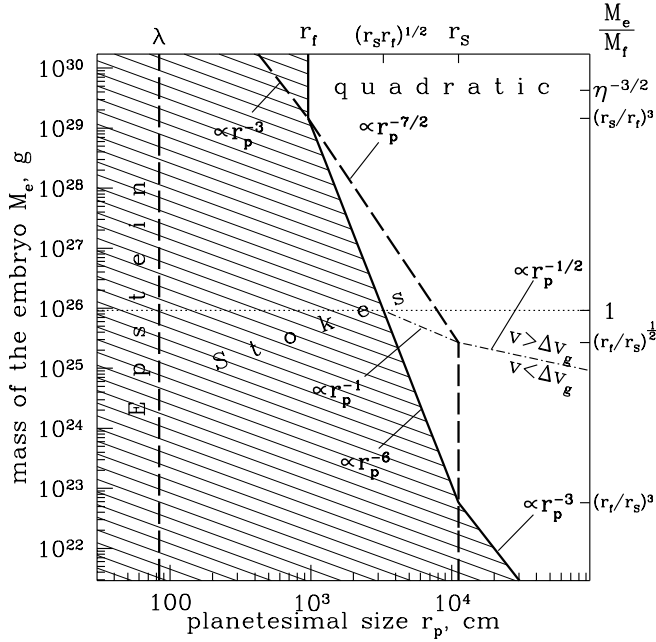


FIG. 5.— Same as Figure 4 but for  $a = 5$  AU (giant planet region), where  $\lambda \lesssim r_f \lesssim r_s$ .

of ice giants. Calculation of boundaries of different gas drag and dynamical regimes is performed using equations (33), (43)-(45), (47). From Figure 3 we can easily see that the molecular mean free path  $\lambda$  is very large in this part of the nebula making the Epstein gas drag important for setting the boundary between the shear- and dispersion-dominated regimes. In this distant part of the nebula only bodies smaller than  $\sim 10$  cm would be dynamically coupled to the gas. Critical planetesimal size below which scattering is shear-dominated is  $50 - 300$  m for embryos with masses  $10^{23} - 10^{27}$  g. This critical size is larger than at 5 AU because gas drag in the Epstein and Stokes regimes is more efficient than in the quadratic regime (for the same  $r_p$  and  $M_e$ ).

### 3.6. Migration, gaps, and multiple embryos.

Conservation of Jacobi constant ensures that any change in the epicyclic energy of planetesimal in the course of its scattering by the embryo is accompanied by the change in planetesimal semimajor axis. As a result, planetesimal surface density distribution gets perturbed by the embryo and a gap might form (Ida & Makino 1993). For the shear-dominated planetesimals gap opening can be especially important, because in this dynamical regime planetesimal guiding centers are moved away from the embryo's orbit by  $\sim R_H$  in a single passage at  $h \approx R_H$ , see (23) (Rafikov 2001). If this happens, accretion of planetesimals by the embryo can be severely affected (Rafikov 2003a).

At the same time, gas drag causes orbital decay of planetesimals between encounters — they migrate towards the Sun. This drift moves planetesimals which are located inside of the embryo's orbit further from it, facilitating the gap opening. On the other hand, on the outer side of the embryo's orbit gas drag causes planetesimals to drift *towards* the embryo, and this tends to

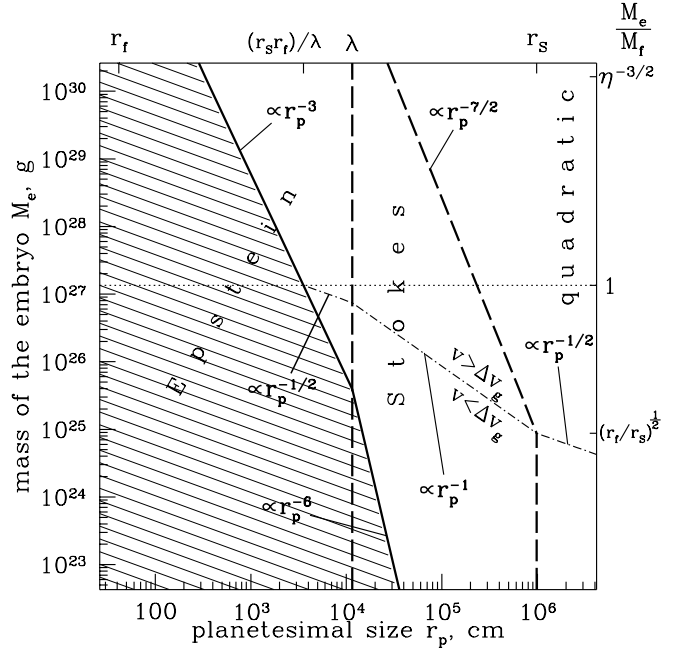


FIG. 6.— Same as Figure 4 but for  $a = 30$  AU (region of ice giants), where  $r_f \lesssim \lambda \lesssim r_s$ .

oppose the gap formation. As long as planetesimals are less massive than the embryo, they are all repelled by scattering in the same way independent of their masses. Thus, the question of whether the gap outside of the embryo's orbit is cleared or not depends only on the damping timescale; there exists a critical size  $r_{mig}$  such that planetesimals of this size initially at  $h \sim R_H$  from the embryo, after being repelled by roughly  $R_H$ , can migrate back the same distance in a synodic period. Only these planetesimals would be accreted by an isolated embryo: planetesimals with  $r_p \gtrsim r_{mig}$  are too big to be brought back to the embryo by the gas drag, and a gap forms preventing their further accretion. Planetesimals smaller than  $r_{mig}$  migrate so fast that in a synodic period they cross the embryo's orbit and are lost to the inner disk. Embryo's accretion would then be rather inefficient as well.

These problems arise only for an *isolated* protoplanetary core. However, during the intermediate stages of planet formation as a consequence of oligarchic growth (Kokubo & Ida 1998) there would be *many* embryos present in a disk at the same time. Their orbits should not be very widely separated: even if it were the case initially, subsequent increase in the embryo masses caused by the accretion of planetesimals would make these separations not too large (see below) in terms of their Hill radii (because  $R_H$  expands as embryo's mass increases, see [20]) and this is what is important for the dynamics.

When such a "crowded" population of protoplanetary cores (which is a natural outcome of oligarchic growth) is present in the disk, gap formation is no longer an issue: although a particular embryo repels planetesimals and tends to open a gap, scattering by another nearby embryo pushes planetesimals back and spatially homogenizes them before they approach the first embryo again. Gap formation is thus suppressed and accretion can pro-



ceed almost uninhibited. On the other side of the problem, although small shear-dominated planetesimals migrate through the orbit of some particular embryo because of the gas drag, there are many other embryos in the inner disk which scatter planetesimals back and forth, so that their inward drift looks more like a random walk through the nebula. In the course of such a diffusion through the protoplanetary disk planetesimals have a high chance of being accreted by one of the many embryos (as long as planetesimals stay in the shear-dominated regime, see §6).

At a glance, it seems improbable that embryos can remain on purely circular and uninclined orbits in a “crowded” configuration because at small radial separations they would strongly scatter each other and very quickly excite large random velocities. However, one should remember that in the course of oligarchic growth most of the solid mass is locked up in planetesimals and not in embryos. This is true until  $M_e$  reaches the isolation mass  $M_{iso}$  defined as

$$M_{iso} \approx M_\odot (4\pi\Sigma_p a^2/M_\odot)^{3/2} \approx 6 \times 10^{26} g a_{AU}^{3/4} \quad (50)$$

if embryos grow predominantly by accretion of shear-dominated planetesimals and

$$\begin{aligned} M_{iso} &\approx M_\odot (4\pi\Sigma_p a^2/M_\odot)^{3/2} (V/\Omega R_H)^{3/2} \\ &\approx 6 \times 10^{26} g (V/\Omega R_H)^{3/2} a_{AU}^{3/4} \end{aligned} \quad (51)$$

if embryo growth is dominated by accretion of large dispersion-dominated planetesimals with typical random velocity  $V$  (e.g. see Rafikov 2003b). Massive planetesimal population exerts *dynamical friction* on embryos transferring random energy of their epicyclic motion to planetesimals, which keeps embryo eccentricities small (see Kokubo & Ida 1995). Planetesimal velocities, in turn, are damped by the gas drag<sup>4</sup> which allows dynamical friction to continue being effective.

Planetesimal disks have presumably contained both massive dispersion-dominated planetesimals and small shear-dominated bodies at the same time. We will assume that the latter comprise some fraction  $\chi < 1$  of the total planetesimal surface density  $\Sigma_p$ . One can show (Stewart & Ida 2000; Rafikov 2003c) that these two populations of planetesimals damp random velocity  $v_e$  of protoplanetary cores at a rate

$$\begin{aligned} \frac{dv_e^2}{dt} &\approx -\Omega v_e^2 \left( \frac{M_\odot}{M_e} \right)^{1/3} \frac{\Sigma_p a^2}{M_\odot} \\ &\times \left[ \chi + (1 - \chi) \left( \frac{\Omega R_H}{V} \right)^4 \right], \end{aligned} \quad (52)$$

where second term represents the contribution of large dispersion-dominated planetesimals (we are dropping here all constant factors and the Coulomb logarithm), while the first term is due to the small shear-dominated bodies<sup>5</sup>. Evidently, small bodies are more important

<sup>4</sup> In the end, the energy of the embryo’s epicyclic motion gets damped by the gas drag, with planetesimal population acting as an intermediary.

<sup>5</sup> Effect of dynamical friction by the shear-dominated bodies can be obtained from that caused by the dispersion-dominated planetesimals by setting  $v = \Omega R_H$  and reducing planetesimal surface density by a factor of  $\chi$ .

for “cooling” the cores than large planetesimals provided that

$$\chi \gtrsim \left( \frac{\Omega R_H}{V} \right)^4. \quad (53)$$

Note that because  $V \gtrsim \Omega R_H$  this inequality can be fulfilled for rather small  $\chi$  (e.g. for  $\chi = 0.02$  for  $V = 3\Omega R_H$ ). In the case opposite to (53) dynamical friction on the protoplanetary cores is controlled by the large dispersion-dominated planetesimals.

We demonstrate later in §6 that the relative importance of shear- or dispersion-dominated populations for the growth of mass of protoplanetary cores is determined by a condition different from (53). Namely, protoplanetary cores grow predominantly through the accretion of small shear-dominated bodies whenever

$$\chi \gtrsim p^{1/2} (\Omega R_H/V)^2, \quad (54)$$

where parameter  $p \ll 1$  is defined by equation (78). In this accretion regime one can also demonstrate that radial separation of embryos  $h \approx R_H$  and their gravitational scattering has a discrete character: random velocities of embryos are strongly excited during their close approaches to each other, but dynamical friction tends to damp them before the next encounter occurs; this is similar to scattering of the shear-dominated planetesimals in the presence of gas drag (see §3.3.1-3.3.4). A particular embryo grows mainly by accretion of material (small planetesimals) from the annulus around its orbit (the so called “feeding zone”) with the radial width  $\approx R_H$  leading to isolation mass in the form (50). For a system of embryos to remain most of the time on uninclined<sup>6</sup> and roughly circular orbits with radial spacing  $h \approx R_H$ , dynamical friction timescale  $t_{df}$  must be shorter than the average time between the embryo encounters  $t_{syn}$  given by (37). Estimating  $t_{df}$  from (52) one can find that this is possible only for embryos with masses satisfying

$$\begin{aligned} M_e &\lesssim M_{e,cr} = M_\odot \left( \frac{\Sigma_p a^2}{M_\odot} \right)^{3/2} \\ &\times \left[ \chi + (1 - \chi) \left( \frac{\Omega R_H}{V} \right)^4 \right]^{3/2}. \end{aligned} \quad (55)$$

Note that if the whole planetesimal disk is shear-dominated, i.e.  $\chi = 1$ , then embryos can stably stay on closely packed ( $h \approx R_H$ ) almost circular and uninclined orbits all the way until they reach the isolation mass (modulo constant factors), compare with (50). However, if  $\chi < 1$  critical embryo mass goes down compared to  $M_{iso}$ .

Whenever the amount of solid mass in shear-dominated planetesimals is so small that (54) is violated and  $\chi \lesssim p^{1/2} (\Omega R_H/V)^2$ , core growth is determined mainly by the accretion of large dispersion-dominated planetesimals. One can demonstrate in this regime that as a result of oligarchic growth radial separations of protoplanetary cores become  $\approx V/\Omega$  (Ida & Makino 1993; Kokubo & Ida 1998) which is larger than  $R_H$ . Feeding zones of embryos are larger than in the shear-dominated case:

<sup>6</sup> Analogous to the planetesimal case, the shear-dominated scattering of embryos by embryos is very inefficient in exciting vertical velocities.

dispersion-dominated planetesimals can be accreted from within  $V/\Omega$  in the radial direction (i.e. the width of the feeding zone is again roughly equal to the radial separation between the embryo orbits). Since orbits of embryos are well separated ( $h \approx V/\Omega \gtrsim R_H$ ) their gravitational scattering is not so dramatic as in the case corresponding to (54) and eccentricity growth has a character of a random walk. Using equation (22) and the fact that embryos encounter their neighbors roughly once every  $t_{syn}(R_H/h) \approx t_{syn}(\Omega R_H/V)$  (where  $t_{syn}$  is defined by [37]) we find growth rate of random velocity to be

$$\begin{aligned} \frac{dv_e^2}{dt} &\approx (\Omega a)^2 \left(\frac{M_e}{M_\odot}\right)^{2/3} \left(\frac{R_H}{h}\right)^4 \times \Omega \left(\frac{M_e}{M_\odot}\right)^{1/3} \frac{h}{R_H} \\ &\approx \Omega(\Omega a)^2 \frac{M_e}{M_\odot} \left(\frac{\Omega R_H}{V}\right)^3. \end{aligned} \quad (56)$$

For the system of embryos to be dynamically stable, the equilibrium value of random velocity  $v_e$  (obtained by balancing scattering rate [56] with the damping due to the dynamical friction [52]) has to be less than  $V$  — orbits of cores should not cross. One can easily find that this is possible only provided that

$$\begin{aligned} M_e &\lesssim M_{e,cr} = M_\odot \left(\frac{\Sigma_p a^2}{M_\odot}\right)^{3/2} \left(\frac{V}{\Omega R_H}\right)^{3/2} \\ &\times \left[1 - \chi + \chi \left(\frac{V}{\Omega R_H}\right)^4\right]^{3/2}, \end{aligned} \quad (57)$$

If planetesimal disk contains only dispersion-dominated planetesimals, i.e.  $\chi = 0$ , then population of embryos can be dynamical stable only until embryos reach corresponding  $M_{iso}$  given by (51). In Figure 7 we display different regimes of dynamical friction and planetesimal accretion as a function of  $\chi$  and  $V/\Omega R_H$ .

Thus, whenever planetesimal disk is one-component (i.e. has either only shear-dominated or only dispersion-dominated planetesimals), it is the isolation mass that sets a limit on the maximum core mass below which protoplanetary cores co-exist on closely spaced but dynamically cold orbits. However in the more realistic case of a disk consisting of both populations (i.e.  $0 < \chi < 1$ ) dynamical stability is violated at masses smaller (sometimes much smaller) than  $M_{iso}$ , as equations (55) and (57) clearly demonstrate. For instance, let us consider the region of giant planets at  $a = 5$  AU where  $p \approx 10^{-3}$  according to (78). Assuming that most of the surface density is in large, 1-km size planetesimals, we find their random velocity  $V \approx 2.2\Omega R_H$  to be set by quadratic gas drag (26). Then, whenever the mass fraction of small shear-dominated planetesimals forming almost two-dimensional subdisk is  $\chi \lesssim 6 \times 10^{-3}$ , both core accretion rate and dynamical friction are set only by large planetesimals. For such small  $\chi$  the system of embryos is dynamically stable until  $M_e$  reaches the isolation mass (51), see (57). For  $6 \times 10^{-3} \lesssim \chi \lesssim 4 \times 10^{-2}$  situation is different: dynamical friction acting on cores is still determined by large planetesimals but core accretion rate is now set by the abundance of small bodies. Orbits of embryos accreting small bodies tend to get closely packed<sup>7</sup>

<sup>7</sup> When  $\chi$  passes through the value  $p^{1/2}(\Omega R_H/V)^2$  equilibrium radial separation between the embryo orbits discontinuously changes from  $V/\Omega$  to  $R_H$ .

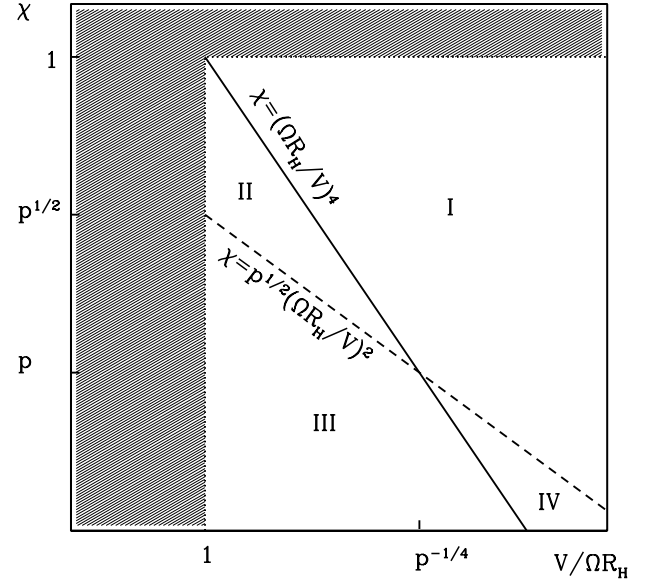


FIG. 7.— Different regimes of core accretion and dynamical friction in the presence of two populations of planetesimals — shear- and dispersion-dominated. Separation of regimes is presented in terms of  $V/\Omega R_H$  — velocity of large planetesimals scaled by the embryo Hill velocity and  $\chi$  — planetesimal mass fraction locked up in small bodies. Solid and dashed lines correspond to conditions (53) and (54).

and this increases gravitational scattering between them. As a result, dynamical instability sets in at a considerably smaller mass  $M_{e,cr} \approx M_{iso}(\Omega R_H/V)^6$ , where  $M_{iso}$  is now given by (50); for  $V = 2.2\Omega R_H$  one finds  $M_{e,cr} \approx 0.01M_{iso}$ . Finally, when  $\chi \gtrsim 4 \times 10^{-2}$  both dynamical friction and core accretion rates are determined by small shear-dominated bodies and  $M_{e,cr} \approx M_{iso}\chi^{3/2}$ , ( $M_{iso}$  is again given by [50]); only when  $\chi = 1$  can instability be postponed until  $M_e$  reaches  $M_{iso}$ .

From this example one can see that the situation in two-component planetesimal disks is very different from that in one-component disks. Even small admixture of shear-dominated planetesimals can completely change the dynamics of a system of protoplanetary cores. Thus, it becomes especially important to know the exact value of  $\chi$  and to follow its evolution in time. Table 1 briefly summarizes our findings by delineating the conditions under which shear-dominated or dispersion-dominated planetesimals control core accretion and dynamical friction.

As cores grow, their Hill radii increase and feeding zones overlap leading to occasional mergers of cores. This keeps their orbital separations from becoming too small but does not lead to dynamical instability because of the dynamical friction. Thus, the overall picture of oligarchic growth described above is not affected by mergers of embryos. However, as soon as  $M_e$  increases beyond the threshold given by (55) or (57), dynamical friction can no longer keep embryos on kinematically cold orbits, their eccentricities and inclinations start to grow, and cores finally switch into the dispersion-dominated regime with respect to each other. Similar effect has been observed by Kokubo & Ida (1995) in N-body simulations,

although they were dealing with the gas-free environment which made dynamical friction less effective since planetesimals were dynamically hot. In this work we are not going to follow this more violent stage of planetesimal disk evolution.

#### 4. LOWER LIMIT ON PLANETESIMAL VELOCITY.

We have demonstrated in §3.3.1 that planetesimal random velocity in the shear-dominated case rapidly decays as a result of gas drag after scattering by the embryo. If the damping time  $t_d$  is much shorter than the time between encounters, planetesimal velocity right before the next approach to the embryo would essentially be zero [ $\propto \exp(-t_{syn}/t_d)$  to be more exact]. As a result, any subdominant sources of stirring which would normally be negligible become important in maintaining random motions at a finite value. These effects then determine the floor below which planetesimal random velocity cannot drop. Here we identify two such effects — scattering by the distant embryos and stirring by the large dispersion-dominated planetesimals — which determine the minimum horizontal and vertical random velocities of planetesimals respectively. We consider these two processes separately.

As we demonstrated in §3.3.6, proto-Solar nebula should contain a population of dynamically cold embryos separated by roughly  $R_H/N$  — we parametrize the uncertainty in the radial separation of cores by the number of embryos  $N$  per  $R_H$  in radius; if cores grow mainly through accretion of shear-dominated planetesimals  $N \approx 1$ , while if they mostly accrete dispersion-dominated bodies  $N \approx (\Omega R_H/V) < 1$ , see §3.3.6. Surface number density of embryos is  $\approx N/(2\pi a R_H)$ .

Distant embryos scatter a given planetesimal quite frequently because both the velocity of incoming embryos (which is determined by the shear in the disk) and their number increase linearly with the radial separation  $h$ . As a result, although scattering by the nearest embryos is discrete, scattering by the cores more distant than some critical  $h_c$  should be considered as a continuous process, similar to the scattering in the dispersion-dominated regime. To determine  $h_c$  we notice that scattering switches from the discrete to continuous mode when the average time between the passages of embryos separated from a given planetesimal by less than  $h_c$  becomes shorter than the typical timescale on which planetesimal velocity would evolve otherwise. For planetesimals with  $r_p \gtrsim r_{stop}$  this typical timescale is the gas damping timescale<sup>8</sup>  $t_d$ .

The rate  $\Gamma(h_c)$  at which embryos with  $|h| < h_c$  pass a particular planetesimal due to the shear in the disk is

$$\Gamma(h_c) = \frac{3\Omega}{2} \frac{N}{2\pi a R_H} \int_{-h_c}^{h_c} |h| dh = \Omega \frac{3}{4\pi} \frac{N}{a R_H} h_c^2. \quad (58)$$

Boundary between the discrete and continuous scattering

<sup>8</sup> Note that for planetesimals smaller than  $r_{stop}$  gas damping time is shorter than  $\Omega^{-1}$ . However the duration of the gravitational interaction with the distant embryo is always  $\sim \Omega^{-1}$  meaning that the typical velocity evolution timescale for planetesimals with  $r_p \lesssim r_{stop}$  is not  $t_d$  but rather  $\Omega^{-1}$ . This, however, is only important for very small planetesimals,  $r_p \lesssim 1$  m (see Figure 3), which are not covered by this study anyway.

is given by  $\Gamma(h_c)t_d \approx 1$ , meaning that

$$h_c \approx \left[ \frac{4\pi}{3} \frac{a R_H}{N} (\Omega t_d)^{-1} \right]^{1/2} = R_H \left( \frac{4\pi}{3N} \frac{t_{syn}}{t_d} \right)^{1/2}. \quad (59)$$

Thus,  $h_c \gg R_H$  for  $N \lesssim 1$  and  $t_d \ll t_{syn}$ .

Scattering by the embryos with  $|h| \gg h_c$  occurs so frequently compared to the gas damping timescale that the random component of scattering averages to zero and eccentricity stirring is given by (22). We find that

$$\begin{aligned} \frac{de^2}{dt} &\approx \frac{3\Omega}{2} \frac{N}{2\pi a R_H} \times 2 \int_0^{h_c} \langle \Delta(e^2) \rangle |h| dh \\ &= 5 \frac{3N}{4\pi} \Omega N \left( \frac{R_H}{a} \right)^3 \left( \frac{R_H}{h_c} \right)^2. \end{aligned} \quad (60)$$

Balancing this stirring by the gas damping  $de^2/dt = -e^2/t_d$  and using (59) we find the equilibrium value of eccentricity

$$e_{min} \approx \sqrt{5} \frac{3N}{4\pi} \frac{R_H}{a} \frac{t_d}{t_{syn}} \sim \frac{R_H}{a} \left( \frac{R_H}{h_c} \right)^2. \quad (61)$$

Using (10)-(12) we evaluate

$$e_{min} \approx 0.04 N \frac{R_H}{a} \left( \frac{M_e}{10^{25} \text{g}} \right)^{1/3} \frac{r_p}{10 \text{ m}} a_{AU}^{5/4}, \quad (62)$$

$$e_{min} \approx 0.03 N \frac{R_H}{a} \left( \frac{M_e}{10^{25} \text{g}} \right)^{1/3} \left( \frac{r_p}{10 \text{ m}} \right)^2 \left( \frac{a_{AU}}{5} \right)^{-5/4} \quad (63)$$

$$e_{min} \approx 0.05 N \frac{R_H}{a} \left( \frac{M_e}{10^{25} \text{g}} \right)^{1/3} \frac{r_p}{10 \text{ m}} \left( \frac{a_{AU}}{30} \right)^{3/2}, \quad (64)$$

for quadratic, Stokes, and Epstein drag regimes respectively. These estimates imply that the minimum horizontal random velocities of small planetesimals are below the Hill velocity, as they should be. For 10 m planetesimals stirred by  $10^{25}$  g embryos  $e_{min}$  corresponds to velocities of the order of  $1 \text{ m s}^{-1}$  in the inner part of the proto-Solar nebula, dropping to  $\approx 0.5 \text{ m s}^{-1}$  at 30 AU.

At the same time, scattering by distant embryos cannot maintain the inclinations of small planetesimals at a finite level. Excitation of the vertical velocity by an encounter with an embryo separated even by  $R_H$  from planetesimal is weakened compared to the excitation of horizontal velocity by the geometric factor  $ia/R_H \ll 1$ . As a result, the growth rate of inclination due to the embryo scattering scales as  $i^2$  (exactly like gas drag) and for  $t_d \lesssim t_{syn}$  gas drag unconditionally dominates. We now consider if stirring by planetesimals (and not embryos) can keep nonzero inclinations of small bodies.

Gas drag acting on planetesimals bigger than 0.1–1 km (depending on the location in the nebula, see §3.3.5) is too weak to prevent them from staying in the dispersion-dominated regime with respect to embryos. Gravitational interaction of these massive planetesimals with small bodies is certain to take place in the dynamically “hot” regime (because for the same physical velocity the Hill radius for the planetesimal-planetesimal scattering is much smaller than  $R_H$  for the embryo-planetesimal scattering).

Rafikov (2003c) has demonstrated that velocity excitation by planetesimals sensitively depends on the

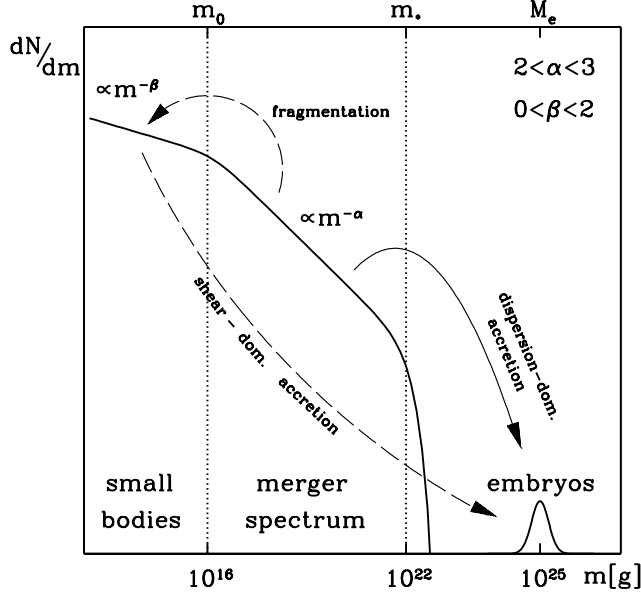


FIG. 8.— Schematic representation of the mass spectrum of solid bodies in the disk (thick solid curve). Three distinct parts of the spectrum can be singled out: small bodies ( $dN/dm \propto m^{-\beta}$ ,  $0 < \beta < 2$ , most of the mass is in biggest objects), merger spectrum ( $dN/dm \propto m^{-\alpha}$ ,  $2 < \alpha < 3$ , most of the mass is in smallest objects), and a set of embryos detached from continuous mass distribution (see §4). Arrows describe different mass transfer routes between the components of the mass spectrum: solid arrow is for the direct accretion of large (dispersion-dominated) planetesimals by embryos, while dashed arrows describe fragmentation of planetesimals with further shear-dominated accretion by embryos. See §7 for more details.

planetesimal mass spectrum. For a given differential surface number density distribution of planetesimal masses  $dN/dm$  the inclination stirring can be written as (Rafikov 2003c)

$$\frac{di^2}{dt} \approx \Omega \left( \frac{\Omega a}{V} \right)^2 \frac{a^2}{M_\odot^2} \int \frac{dN(m)}{dm} m^2 dm, \quad (65)$$

where  $V$  is the random velocity of large dispersion-dominated planetesimals (which we for simplicity set constant, independent of  $m$ ). Shear-dominated planetesimals are not efficient at velocity excitation (but they matter for dynamical friction). Because of the stirring by embryos  $V$  should be some multiple of  $\Omega R_H$ , but owing to the action of gas drag (and planetesimal dynamical friction) it is not higher than several  $\Omega R_H$ , see equations (27), (42), and (46).

Numerical simulations very often produce planetesimal mass spectra such that  $dN/dm \propto m^{-\alpha}$  with  $\alpha \approx 2.5$  within a wide range of masses (Kokubo & Ida 1996). In a disk with such spectrum most of the mass is concentrated at the lower end of distribution while most of the stirring is done by its upper end (Rafikov 2003c). We will assume that planetesimal mass spectrum has this form for  $m_0 \lesssim m_p \lesssim m_*$ , where we somewhat arbitrarily take  $m_0 = 10^{16}$  g and  $m_* \approx 10^{22}$  g (roughly 1-km and 100-km size planetesimals); see Figure 8 for a schematic picture of the assumed size distribution. Excitation of inclination by the largest planetesimals ( $m_p \approx m_*$ , which are

still much smaller than the embryos) can be expressed in terms of  $m_0$ ,  $m_*$ , and planetesimal surface mass density  $\Sigma_p$  (dominated by planetesimals with  $m_p \approx m_0$ ) roughly as (Rafikov 2003c)

$$\frac{di^2}{dt} \approx \Omega \left( \frac{\Omega a}{V} \right)^2 \frac{m_0 \Sigma_p a^2}{M_\odot^2} \left( \frac{m_*}{m_0} \right)^{3-\alpha}. \quad (66)$$

In writing down this expression we have assumed that large planetesimals are numerous enough to give rise to a continuous rather than discrete stirring. Balancing (66) with  $-i^2/t_d$  we find the equilibrium value of inclination:

$$i_{min} \approx \frac{\Omega a}{V} \left[ \Omega t_d \frac{m_0 \Sigma_p a^2}{M_\odot^2} \left( \frac{m_*}{m_0} \right)^{3-\alpha} \right]^{1/2}. \quad (67)$$

Evaluating this expression for  $V = 3\Omega R_H$ ,  $M_e = 10^{25}$  g,  $\Sigma_p$  given by (2),  $t_d$  given by (10)-(12), and our adopted values of  $m_0$ ,  $m_*$ , and  $\alpha = 2.5$  we find that

$$i_{min} \approx 10^{-4} \frac{R_H}{a} \left( \frac{r_p}{10 \text{ m}} \right)^{1/2} a_{AU}^{7/8}, \quad (68)$$

$$i_{min} \approx 10^{-4} \frac{R_H}{a} \frac{r_p}{10 \text{ m}} \left( \frac{a_{AU}}{5} \right)^{-3/8}, \quad (69)$$

$$i_{min} \approx 3 \times 10^{-4} \frac{R_H}{a} \left( \frac{r_p}{10 \text{ m}} \right)^{1/2} \frac{a_{AU}}{30}, \quad (70)$$

for corresponding gas drag regimes. These values of inclination correspond to very small vertical velocities of planetesimals,  $\sim 1 \text{ cm s}^{-1}$  in the vicinity of  $10^{25}$  g protoplanetary cores at 30 AU. Evidently, since  $i_{min} \ll e_{min}$  (see [62]-[64]) this type of stirring would not be able to affect minimum eccentricities of planetesimals.

Scattering by large planetesimals would vertically perturb not only small bodies but also embryos. Balancing the stirring rate (66) with the dynamical friction rate (52), we find that the minimum inclination of the embryo  $i_{e,min}$  is about

$$\begin{aligned} i_{e,min} &\approx \frac{R_H}{a} \left( \frac{V}{\Omega R_H} \right) \left[ \frac{m_0}{M_e} \left( \frac{m_*}{m_0} \right)^{3-\alpha} \right]^{1/2} \\ &\times \left[ 1 + \chi \left( \frac{V}{\Omega R_H} \right)^4 \right]^{-1/2} \\ &\approx 10^{-3} \frac{R_H}{a} \left( \frac{V}{\Omega R_H} \right) \left( \frac{M_e}{10^{25} \text{ g}} \right)^{-1/2} \left[ 1 + \chi \left( \frac{V}{\Omega R_H} \right)^4 \right]^{-1/2}, \end{aligned} \quad (71)$$

provided that the time between encounters with large planetesimals (which dominate vertical stirring) is shorter than  $t_{df}$  (for continuous approximation to hold). As a bottom line, we may conclude that scattering by large planetesimals keeps inclinations of small bodies relative to protoplanetary cores at the level of  $\sim 10^{-3}(R_H/a)$ , most likely via the stirring of cores.

There are other possibilities for maintaining inclinations of shear-dominated planetesimals at some minimum level. One of them is the gravitational scattering between small bodies themselves which transfers the energy of random motion from horizontal into the vertical direction. This is likely not to be important because dynamical relaxation of small bodies is very slow. Another possibility is a gravitational instability in the thin layer

(P. Goldreich, private communication) which may excite random velocities of small constituent bodies. Assuming that a fraction  $\chi$  of solid mass is locked up in small shear-dominated bodies, one can find that instability would operate if the planetesimal velocity dispersion is below  $\chi\pi G\Sigma_p/\Omega \approx 30 \text{ cm s}^{-1} \chi$  (usual Toomre criterion), and this is still below  $e_{min}\Omega a$  even for  $\chi = 1$ . Finally, inelastic collisions between small planetesimals can heat the disk vertically, and we elaborate more on this in the next section.

### 5. INELASTIC COLLISIONS.

Inelastic collisions between planetesimals act as efficient source of damping. The escape speed from the surface of a 100 m body is about  $10 \text{ cm s}^{-1}$  and planetesimals are typically moving with higher velocities (see [62]-[64]), which means that (a) they would lose a lot of energy in high-energy collisions, and (b) gravitational focusing is unimportant and collision cross-section is almost equal to the geometric cross-section of colliding bodies. Assuming that planetesimals lose a fraction  $\sim 1$  of their energy when they collide, we estimate the velocity damping in inelastic collisions to be given by

$$\frac{dv^2}{dt} \approx -\Omega v^2 \frac{\chi \Sigma_p}{\rho_p r_p} \frac{v_h}{v_z}, \quad (72)$$

where we have again assumed that only a fraction  $\chi$  of solid mass is in the shear-dominated planetesimals. From this expression it is clear that inelastic collisions lead to exponential damping of velocity (if  $v_h/v_z \approx \text{const}$ ) on a timescale

$$t_{inel} \equiv \Omega^{-1} \chi^{-1} (\rho_p r_p / \Sigma_p) (v_z / v_h) \\ \approx 5 \text{ yr } \chi^{-1} (v_z / v_h) \frac{r_p}{10 \text{ m}} a_{AU}^3. \quad (73)$$

Importance of inelastic collisions is judged by comparing  $t_{inel}$  with  $t_d$  — damping time due to the gas drag. Using equations (10)-(12) we find

$$t_d / t_{inel} \approx 0.25 \chi (v_h / v_z) a_{AU}^{-1/4}, \quad (74)$$

$$t_d / t_{inel} \approx 0.1 \chi (v_h / v_z) \left( \frac{r_p / \lambda}{10} \right), \quad (75)$$

$$t_d / t_{inel} \approx 0.01 \chi (v_h / v_z), \quad (76)$$

for quadratic, Stokes, and Epstein gas drag regimes. These estimates clearly demonstrate that  $t_d \lesssim t_{inel}$  whenever  $v_z \sim v_h$  ( $i \sim e$ ), meaning that inelastic collisions are unimportant when planetesimal velocities are roughly isotropic. This is always true in the dispersion-dominated regime allowing us to neglect inelastic collisions in this case.

Situation is different in the shear-dominated regime where one can easily have  $v_z \ll v_h$  (see §4). Let's assume that planetesimal inclination right before the encounter with some embryo is very low. Right after the scattering event inclination remains roughly the same (see [24]) while eccentricity goes up to  $\sim (R_H/a) \gg i_{min}$ ; as a consequence,  $t_{inel}$  immediately becomes much shorter than  $t_d$  and inelastic collisions suddenly become more important than gas drag. However, this is a very transient stage because inelastic collisions not only dissipate energy but also isotropize the velocities of colliding bodies. If planetesimals were colliding like rigid balls, bouncing

off after collision, one would expect roughly isotropic recoil velocities. Consequently, one would expect  $v_z \approx v_h$  after every planetesimal has experienced a single physical collision, i.e. after time  $t_{inel}$  has passed since the scattering by the embryo. This immediately reduces the importance of inelastic collisions and makes gas drag more important again for the random velocity dissipation shortly after scattering has occurred, see (74)-(76).

After that, according to (49), inclination decays slower than eccentricity does meaning that the role of inelastic collisions keeps decreasing. If the time interval between the successive encounters with the embryo is long enough, the eccentricity decay will stop at the asymptotic value  $e_{min}$  (of course, with occasional oscillations due to scattering by distant embryos) while the inclination would continue to decay further until it reaches  $i_{min} \ll e_{min}$ . At this stage  $v_z/v_h$  goes down and physical collisions can again start occurring quite frequently; however, the imminent isotropization of velocities after every collision limits their importance (in comparison with that of the gas drag) only to short periods of time. As a result, the timescale of velocity damping between encounters with embryos should still be very close to the gas damping time scale  $t_d$ .

Physical collisions might affect the determination of  $i_{min}$  since they can be effective at pumping the energy of horizontal motions into vertical ones. The minimum velocity anisotropy  $v_z/v_h$  they provide can be determined from the condition  $t_d/t_{inel} \approx 1$  and turns out to be roughly  $0.25\chi$ ,  $0.1\chi$ , and  $0.01\chi$  for typical parameters of quadratic, Stokes, and Epstein drag regimes, see equations (74)-(76). Scattering by distant embryos maintains horizontal random velocities of small planetesimals at the level given by (62)-(64), and this degree of anisotropy results in  $i_{min} \approx (v_z/v_h)e_{min}$  which for 10 m planetesimals is about  $0.01\chi(R_H/a)$  at 1 AU and  $5 \times 10^{-4}\chi(R_H/a)$  at 30 AU. Comparing this with (68)-(70) and (72) we may conclude that for not too small values of  $\chi$  ( $\gtrsim 0.1$ ) inelastic collisions are important for setting the minimum value of relative embryo-planetesimal inclination in the presence of gas drag in quadratic or Stokes regimes (in the inner parts of the proto-Solar nebula, inside 5 – 10 AU). Whenever shear-dominated planetesimals are affected by the gas drag in the Epstein regime, inelastic collisions can compete with stirring by large planetesimals only for  $\chi \approx 1$ .

This discussion has assumed rather idealized model of planetesimal collisions (rigid balls). In reality high-energy impacts are likely to be catastrophic, leading to the disruption of participant bodies. Then the amount of kinetic energy transferred into vertical motions and the degree of isotropization would be determined by the ejection velocities of resulting debris. Observations of velocity dispersions in collisional families of asteroids (Zappala et al. 1996) and results of numerical simulations (Michel et al. 2003) indicate that ejection velocities are considerably smaller than the initial planetesimal velocities. This slows down the velocity isotropization compared to the case of collisions of “hard balls”. Nevertheless, we do not expect this to seriously change the general picture outlined before. Besides, it is not at all clear how anisotropic would ejection velocities be in the case of planetesimals (10-100 m in size, strength-dominated fragmentation) colliding at several tens of  $\text{m s}^{-1}$ , since collisions between

10-km asteroids (gravity-dominated fragmentation), on which information exists, occur at relative speeds of several  $\text{km s}^{-1}$ .

#### 6. ACCRETION OF LOW-ENERGY PLANETESIMALS.

Protoplanetary embryos grow by accreting planetesimals. Accretion in differentially rotating disks is intrinsically complicated because of the three-body gravitational interaction of the two merging bodies and the central mass. One can however greatly simplify this problem by treating accretion as a two-body process while approximately taking into account three-body effects by limiting from below planetesimal approach velocity relative to the embryo by  $\Omega R_H$ . This is a direct consequence of the shear present in the disk.

With this in mind we can write a rather general formula for the protoplanetary mass accretion rate:

$$\begin{aligned} \frac{dM_e}{dt} &\approx n_p m_p R_e^2 v_a \left(1 + \frac{v_{esc}^2}{v_a^2}\right) \\ &\approx \Omega \Sigma_p R_H^2 \frac{R_e}{R_H} \frac{v_a}{v_z} \left(\frac{\Omega R_H}{v_a}\right)^2, \end{aligned} \quad (77)$$

where  $R_e$  is the physical size of the embryo and the last equality holds for  $v_a \ll v_{esc}$ . Dimensionless physical size of the core  $p$  relative to its Hill radius is independent of the core mass but varies with the distance from the Sun:

$$p \equiv \frac{R_e}{R_H} = \left(\frac{3}{4\pi} \frac{M_\odot}{\rho_p a^3}\right)^{1/3} \approx 5.2 \times 10^{-3} a_{AU}^{-1}. \quad (78)$$

Clearly,  $R_e \ll R_H$  and  $p \ll 1$ .

Scattering of planetesimals by the embryo in the dispersion-dominated regime always tends to maintain  $v_z \approx v \approx v_a \gtrsim \Omega R_H$ , thus

$$\frac{dM_e}{dt} \approx \Omega p \Sigma_p R_H^2 \left(\frac{\Omega R_H}{v}\right)^2. \quad (79)$$

In the shear-dominated regime approach velocity  $v_a$  is almost independent of planetesimal eccentricity or inclination and is  $\approx \Omega R_H$ . At the same time, vertical velocity of planetesimals  $v_z$  setting the thickness of planetesimal disk is smaller than  $\Omega R_H$ , and we find that

$$\frac{dM_e}{dt} \approx \Omega p \Sigma_p R_H^2 \frac{\Omega R_H}{v_z}. \quad (80)$$

Derivation of equation (77) has implicitly assumed that the maximum impact parameter at infinity with which planetesimal can be accreted by the embryo  $R_e \sqrt{1 + v_{esc}^2/v_a^2}$  is smaller than the planetesimal disk thickness  $v_z/\Omega$ . In the shear-dominated case, when  $v_a \sim \Omega R_H$ , this sets a limit on the vertical velocity of planetesimals at which their accretion can still be described by equation (77):

$$v_z \gtrsim v_{z,cr} \equiv p^{1/2} \Omega R_H \approx 0.07 \Omega R_H a_{AU}^{-1/2} \quad (81)$$

(Greenberg et al. 1991; Dones & Tremaine 1993). Equation (80) is applicable only for  $v_z \gtrsim v_{z,cr}$ . Whenever  $v_z \lesssim v_{z,cr}$  planetesimal disk is very thin and embryo can accrete the whole vertical column of material it encounters (eccentricity is only restricted to be smaller than  $R_H/a$ ). In this case one can easily show that

$$\begin{aligned} \frac{dM_e}{dt} &\approx \Omega \Sigma_p R_e R_H \left(1 + \frac{v_{esc}^2}{v_a^2}\right)^{1/2} \\ &\approx \Omega p^{1/2} \Sigma_p R_H^2. \end{aligned} \quad (82)$$

This is the highest possible accretion rate of planetesimals by the protoplanetary core that can be achieved in the planetesimal disk.

It is possible that most of the planetesimal mass has been concentrated in bodies with sizes of about 1 – 10 km (merger products in Figure 8) which interact with embryos in the dispersion-dominated regime. According to (79) the growth timescale of the embryo due to the accretion of these bodies is

$$\begin{aligned} t_{g,dd} &\approx \Omega^{-1} \left(\frac{M_e}{M_\odot}\right)^{1/3} \frac{M_\odot}{\Sigma_p a^2} \frac{R_H}{R_e} \left(\frac{v}{\Omega R_H}\right)^2 \\ &\approx 10^5 \Omega^{-1} \left(\frac{M_e}{10^{25} \text{g}}\right)^{1/3} \left(\frac{v}{\Omega R_H}\right)^2 a_{AU}^{1/2}. \end{aligned} \quad (83)$$

Using equations (27), (42), and (46) we find that the time needed to build  $10^{25}$  g protoplanetary core by accretion of such dispersion-dominated planetesimals is  $\approx 10^5$  yr at 1 AU,  $\approx 4 \times 10^6$  yr at 5 AU, and  $\approx 3 \times 10^7$  yr at 30 AU.

At the same time, as we hypothesized in §3.3.6 a fraction  $\chi < 1$  of planetesimal mass could have been in small bodies which are shear-dominated with respect to embryos. This mass is concentrated in a vertically thin population and comparing (68)-(70) & (72) with (81) we find vertical velocity of planetesimals in the subdisk to be smaller than  $v_{z,cr}$ . Thus, small shear-dominated bodies can be very efficiently consumed by embryos, and we find using (82) that the embryo's growth timescale due to their accretion is

$$\begin{aligned} t_{g,sd} &\approx \chi^{-1} \Omega^{-1} \left(\frac{M_e}{M_\odot}\right)^{1/3} \frac{M_\odot}{\Sigma_p a^2} \left(\frac{R_H}{R_e}\right)^{1/2} \\ &\approx 7 \times 10^3 \chi^{-1} \Omega^{-1} \left(\frac{M_e}{10^{25} \text{g}}\right)^{1/3}. \end{aligned} \quad (84)$$

This is  $\approx 10^3 \chi^{-1}$  yr at 1 AU,  $\approx 10^4 \chi^{-1}$  yr at 5 AU, and  $\approx 2 \times 10^5 \chi^{-1}$  yr at 30 AU. Thus, even if only about 1% of the mass in solids is locked up in the shear-dominated planetesimals ( $\chi = 10^{-2}$ ) they would still dominate the accretion rate of the embryo because  $t_{g,sd} \lesssim t_{g,dd}$ ! Comparing (79) and (82) with  $\Sigma_p$  lowered by a factor of  $\chi$  we find that accretion of small shear-dominated bodies from very thin disk is more important for embryo growth than accretion of large dispersion-dominated planetesimals whenever  $\chi$  is such that condition (54) is fulfilled.

#### 7. DISCUSSION.

The outlined picture of planetesimal dynamics in the gaseous nebula naturally divides planetesimals of different sizes into two well-defined populations with respect to gravitational scattering by a set of protoplanetary cores. One is a “hot” population of bodies bigger than 0.1–1 km which interact with embryos in the dispersion-dominated regime and have large inclinations so that their scattering is an intrinsically three-dimensional process. The other is a “cold” population of smaller planetesimals (sizes below 0.1–1 km) which interact with embryos in the shear-dominated regime. These planetesimals tend to be confined by the action of the gas drag to a vertically thin disk [with a thickness of  $\sim 10^{-3} R_H$ ] near the nebular midplane.

Difference between these populations is most striking when the accretion of planetesimals by the embryos is

concerned. Accretion of dynamically hot planetesimals allows  $10^{25}$  g embryo to double its mass in  $\sim 10^5$  yr in the terrestrial planet region and in several  $10^7$  yr in the region of ice giants. The latter timescale is quite long from the cosmogonical point of view. At the same time, accretion of cold planetesimals is about 100 times faster, with mass doubling timescale of  $\sim 10^3$  yr and  $\sim 10^5$  yr in the inner and outer parts of the nebula, provided that *all* solid mass is locked in these small planetesimals. Formation of gaseous atmospheres around massive protoplanetary cores further accelerates accretion of small bodies: gaseous envelopes can be very efficient at trapping small planetesimals (Inaba & Ikoma 2003), thus increasing the capture radius  $R_e$  and shortening the growth timescale. Protoplanetary cores would also grow by merging with other cores (since in our picture they reside on closely spaced orbits as long as  $M_e \lesssim M_{e,crit}$ , see §3.3.6); apparently, the faster cores grow, the closer their orbits are in the Hill coordinates, and the faster they merge.

It is possible that most of the solid mass in the proto-Solar nebula was concentrated from the very start in small (10 – 100 m) dynamically cold bodies. In this case  $\chi \approx 1$  and growth of embryos should be very fast, see equation (84). It is, however, equally possible that most of the mass was initially locked up in large (1 – 10 km) dispersion-dominated planetesimals and not in the dynamically cold population of small bodies, i.e.  $\chi \ll 1$ . In this case, although there is a huge reservoir of solid mass potentially available for the accretion, embryos can hardly make use of it because hot planetesimals are accreted rather inefficiently, see equation (83). At the same time, cold population which can potentially allow a vigorous growth of the embryo might simply not contain enough surface density to ensure high enough accretion rate (accretion timescale is inversely proportional to the fraction of mass contained in small planetesimals, see [84]). Thus, unless enough mass ( $\chi \gtrsim 10^{-2}$ ) is transferred from hot to cold planetesimals, embryos would grow slowly accreting large dispersion-dominated planetesimals.

A natural process for transferring mass from the big bodies into small ones is planetesimal fragmentation (see Figure 8), which should naturally be taking place in the presence of massive embryos. Indeed, the escape speed from the surface of 1 km body is about  $1 \text{ m s}^{-1}$ , while the Hill velocity of  $10^{25}$  g embryo is  $\approx 50 \text{ m s}^{-1}$  at 1 AU and is  $\approx 10 \text{ m s}^{-1}$  at 30 AU. Thus, 1-km planetesimals possibly containing most of the solid mass in the disk would collide with kinetic energy far exceeding their gravitational binding energy. Depending on their internal strength, parent bodies can be disrupted into a number of smaller fragments in such collisions. Collision strength is likely to be very small for objects in the outer Solar System which are thought to be composed primarily of ices. Comets are presumably the closest existing analogs of distant planetesimals and they are known to have small internal strength, e.g. from observations of tidal disruption of Shoemaker-Levy comet by Jupiter (Greenberg et al. 1995). Thus, it would be natural to expect that collisional fragmentation triggered by the dynamical excitation of planetesimals by massive protoplanetary cores readily occurs at least in the outer Solar System.

Efficiency of fragmentation is set by the collision

timescale  $t_{inel}$  of planetesimals with sizes in which most of the solid mass is concentrated. Using (73) for 1 km bodies with  $\chi = 1$  and  $v_z \approx v_h$  we estimate<sup>9</sup> it to be  $\sim 10^3$  yr at 1 AU and  $\sim 10^7$  yr at 30 AU. This might seem like a rather long timescale in the outer Solar System but one should keep in mind that channeling just 10% of mass into the population of cold planetesimals would increase the embryo's accretion rate by a factor of  $\approx 10$  compared to the accretion of dispersion-dominated bodies, and this can be accomplished in a time 10 times shorter than  $t_{inel}$ , i.e. in about several Myrs. Note that according to (84) the characteristic growth time of  $10^{25}$  g embryo by accretion of small bodies is also several Myrs for  $\chi \approx 0.1$ . Growth time decreases as  $\chi$  gradually goes up meaning that several Myrs is a natural evolution timescale for such embryos in the outer Solar System. We may conclude that if embryos grow mainly by accretion of small planetesimals then the planet formation timescale is intimately related to the timescale of fragmentation of massive planetesimals in catastrophic collisions.

Accretion rate and dynamics of protoplanetary cores would in the end depend on the details of the time evolution of the mass fraction in small planetesimals  $\chi$ , see §3.3.6 and 6. Scaling of  $\chi$  with time would also determine whether inelastic collisions between small planetesimals are an important dynamical factor; as we demonstrated in §5, this can in some cases be an issue in the inner parts of the protoplanetary nebula. The amount of solid material contained in small planetesimals is determined by (1) the input of mass due to the fragmentation of large planetesimals, (2) the removal of mass via the accretion by embryos, and (3) the evolution of the surface density of small planetesimals due to the random scattering by embryos and their inward migration induced by the gas drag (Weidenschilling 1977; Thommes et al. 2003). Self-consistent calculation of  $\chi$  has to combine all these contributions and is beyond the scope of this study.

Rapid accretion of small planetesimals can proceed provided that not only small bodies but also embryos themselves are on almost circular and uninclined orbits. As we have demonstrated in §3.3.6, oligarchic growth allows simultaneous existence of many protoplanetary cores only if cores are lighter than about  $10^{25} - 10^{27}$  g (at 1 AU), since in that case their random motions can be kept small by planetesimal dynamical friction. The exact value of the maximum core mass at which dynamical stability is still possible sensitively depends on the amount of mass concentrated in small shear-dominated bodies, see §3.3.6. After reaching this mass embryos would be dynamically excited ( $e, i \gtrsim R_H/a$ ) and even if small planetesimals can still be kept confined to a cold, thin disk, embryo's accretion would proceed in the dispersion-dominated regime rather slowly (because relative embryo-planetesimal velocity is increased above  $\Omega R_H$ ).

Discrete nature of the shear-dominated scattering of small planetesimals by the embryos is very important for accurate calculation of processes characterized by the energy threshold such as the disruption of small planetes-

<sup>9</sup> Collision timescale would be smaller for small  $v_z/v_h$  (see §4), but this is partly compensated by the burst-like character of the fragmentation process, see below.

imals in catastrophic collisions. Usual continuous approximation suitable in the dispersion-dominated regime would not work in such cases because it characterizes planetesimal velocity by its average value which is either above or below the threshold, meaning that corresponding process is either always on or always off. In reality, planetesimal velocity changes continuously between the encounters with embryos from very large values (about  $\Omega R_H$ ) to very small ones. As a result, planetesimal velocity can be above the threshold for some time and during this period corresponding process would operate (see Figure 2). Later on velocity would drop below the threshold and process would switch off. This is qualitatively different from what one would obtain using continuous description for the planetesimal scattering in the shear-dominated regime. For the fragmentation of small bodies this implies that planetesimal destruction in catastrophic collisions proceeds in bursts right after each passage of the embryo, when relative planetesimal velocities are high, but later on, when velocities are damped by the gas drag, collisions might not be energetic enough to continue fragmenting planetesimals.

## 8. CONCLUSIONS.

We have explored the details of planetesimal dynamics near protoplanetary embryos in the presence of gas drag. We showed that large ( $\gtrsim 1$  km in size) planetesimals are kept in the dispersion-dominated regime as a result of scattering by protoplanetary cores scattering, although their average velocities are reduced by the gas drag. Bodies smaller than roughly 0.1–1 km (depending on the location in the nebula) interact with protoplanetary cores in the shear-dominated regime. Owing to the action of the gas drag these planetesimals settle into a geometrically thin layer near the nebular midplane; between consecutive encounters with the embryos they experience strong velocity damping which allows them to approach embryos every time with the relative velocity comparable to the Hill velocity — minimum velocity which can be achieved in a differentially rotating disk.

For different locations in the proto-Solar nebula we have determined which planetesimals are only weakly affected by the gas drag and are in the dispersion-dominated regime, and which planetesimals are so strongly coupled to the gas that their velocities are below the Hill velocity of the protoplanetary cores. Dynamical peculiarities of the shear-dominated regime in the presence of gas lead to a very high efficiency of accretion of small bodies by the embryos. If the surface mass density of small bodies is high enough ( $\gtrsim 1\%$  of the total sur-

face density in solids) their accretion would dominate the embryo's growth rate (relative to the accretion of more massive, dispersion-dominated planetesimals).

Large planetesimals ( $\gtrsim 1$  km in size) likely containing most of the mass in solids have large random velocities and are not very efficiently accreted by embryos. However, they inelastically collide with each other at high velocities and fragment into smaller pieces contributing to the population of small bodies. Thus, the embryo's growth by accretion of small shear-dominated planetesimals can be regulated by the fragmentation of bigger, dispersion-dominated bodies. Planetesimal fragmentation would probably be easiest in the outer Solar System where colliding bodies are mostly composed of ices and are therefore internally weak and susceptible to easy destruction. The natural timescale for the growth of  $10^{25}$  g protoplanetary embryos by accretion of small planetesimals turns out to be around several Myrs at 30 AU from the Sun. Cores of ice giants can be formed in  $\sim 10^7$  yr after large planetesimals lose all their mass in catastrophic collisions to small debris which can be effectively accreted by massive embryos. This scenario would work only if the population of protoplanetary cores formed as the outcome of oligarchic growth can be kept on almost non-inclined and circular orbits. As we demonstrated in §3.3.6, this is possible only if embryo masses do not exceed a specific limit dictated by the efficiency of planetesimal dynamical friction, which sensitively depends on the planetesimal mass fraction  $\chi$  locked up in small planetesimals and velocity of large dispersion-dominated planetesimals.

Future work should address the issues of the self-consistent evolution of the mass fraction  $\chi$  contained in small bodies; the role of inelastic collisions using improved fragmentation physics (can be an issue in the inner Solar System); the final fate of massive embryos which cannot be kept dynamically cold by the planetesimal dynamical friction, and so on.

I am grateful to Jeremy Goodman for always stressing to me the importance of gas for the planetesimal dynamics. I have greatly benefited from numerous discussions with Peter Goldreich who has been working on similar problems. Useful comments by Yoram Lithwick and Re'em Sari incited additional clarifications in §3.3.6. Author is a Frank and Peggy Taplin Member at the IAS; he is also supported by the W. M. Keck Foundation and NSF grant PHY-0070928.

## REFERENCES

- Adachi, I., Hayashi, C., & Nakazawa, K. 1976, *Prog. Theor. Phys.*, 56, 1756  
 Dones, L. & Tremaine, S. 1993, *Icarus*, 103, 67  
 Greenberg, R., Bottke, W. F., Carusi, A., & Valsecchi, G. B. 1991, *Icarus*, 94, 98  
 Greenberg, J. M., Muzitani, H., & Yamamoto, T. 1995, *A&A*, 295, L35  
 Hasegawa, M. & Nakazawa, K. 1990, *A&A*, 227, 619  
 Hénon, M. & Petit, J. M. 1986, *Celest. Mech.*, 38, 67  
 Ida, S. 1990, *Icarus*, 88, 129  
 Ida, S., Kokubo, E., & Makino, J. 1993, *MNRAS*, 263, 875  
 Ida, S. & Makino, J. 1993, *Icarus*, 106, 210  
 Inaba, S. & Ikoma, M. 2003, *A&A*, 410, 711  
 Kokubo, E. & Ida, S. 1995, *Icarus*, 114, 247  
 Kokubo, E. & Ida, S. 1996, *Icarus*, 123, 180  
 Kokubo, E. & Ida, S. 1998, *Icarus*, 131, 171  
 Landau, L. D. & Lifshitz, E. M. 1987, *Fluid Mechanics*; Pergamon Press  
 Michel, P., Benz, W., & Richardson, D. C. 2003, *Nature*, 421, 608  
 Rafikov, R. R. 2001, *AJ*, 122, 2713  
 Rafikov, R. R. 2003a, *AJ*, 125, 922  
 Rafikov, R. R. 2003b, *AJ*, 125, 942  
 Rafikov, R. R. 2003c, *AJ*, 126, 2529  
 Safronov, V. S. 1969, *Evolution of the Protoplanetary Cloud and Formation of the Earth and Planets*; Nauka, Moscow  
 Stewart, G. R. & Ida, S. 2000, *Icarus*, 143, 28  
 Thommes, E. W., Duncan, M. J., & Levison, H. F. 2003, *Icarus*, 161, 431



TABLE 1. CORE ACCRETION AND DYNAMICAL FRICTION REGIMES.

Region <sup>10</sup> <sub>a</sub>	Conditions	Dyn. friction <sup>11</sup> <sub>b</sub>	Accretion <sup>12</sup> <sub>b</sub>	$M_{e,cr}/M_{iso}$ <sup>13</sup> <sub>c</sub>
I	$\chi > (\Omega R_H/V)^4$ , $p^{1/2}(\Omega R_H/V)^2$	SD <sup>18</sup> <sub>b</sub>	SD	$\chi^{3/2}$
II	$p^{1/2}(\Omega R_H/V)^2 < \chi < (\Omega R_H/V)^4$	DD <sup>19</sup> <sub>b</sub>	SD	$(\Omega R_H/V)^6$
III	$\chi < (\Omega R_H/V)^4$ , $p^{1/2}(\Omega R_H/V)^2$	DD	DD	1
IV	$(\Omega R_H/V)^4 < \chi < p^{1/2}(\Omega R_H/V)^2$	SD	DD	$\chi^{3/2}(V/\Omega R_H)^6$

Wetherill, G. W. & Stewart, G. R. 1989, *Icarus*, 74, 542

Weidenschilling, S. J. 1977, *MNRAS*, 180, 57

Whipple, S. J. 1971, in *From Plasma to Planet*; Almquist & Wiksell, p. 211

Zappala, V., Cellino, A., Dell'oro, A., Migliorini, F., & Paolicchi, P. 1996, *Icarus*, 1996, 124, 156

Roman numerals correspond to different regions in Figure 7. Shows which planetesimal population — dispersion-dominated (DD) or shear-dominated (SD) — dominates dynamical friction and accretion rate of embryos.

$M_{e,cr}$  and  $M_{iso}$  are given by (55) and (50) in regions I & II and (57) and (51) in regions III & IV.

<sup>19</sup> a

<sup>19</sup> b

<sup>19</sup> c